bioRxiv preprint doi: https://doi.org/10.1101/2025.02.03.636213; this version posted February 4, 2025. The copyright holder for this preprint (which was not certified by peer review) is the author/funder, who has granted bioRxiv a license to display the preprint in perpetuity. It is made available under a CC-BY-NC-ND 4.0 International license.

Cross-Species Communication via Fungal Extracellular Vesicles

Renan E. A. Piraine[1], Henrique T. Oliveira[1], Patrick W. Santos[1], Julia L. Froldi[1], Bianca T. M. Oliveira[1], Caroline P. Rezende[2], Gabriel E. S. Trentin[1], Lucas F. B. Nogueira[1], Arnaldo L. Colombo[3], Arturo Casadevall[4], Marcio L. Rodrigues[5], Fausto Almeida[1]

[1]Department of Biochemistry and Immunology, Ribeirão Preto Medical School, University of São Paulo, Ribeirão Preto, São Paulo, Brazil

[2]Department of Molecular Biology, Cancer Molecular Research Laboratory (LIMC)/ FAMERP, São José do Rio Preto, São Paulo, 15090-000, Brazil

[3]Special Laboratory of Mycology, University of São Paulo, São Paulo, São Paulo, Brazil

[4]Department of Molecular Microbiology and Immunology, Johns Hopkins School of Public Health, Baltimore, Maryland, United States

[5]Gene Expression Regulation Laboratory, Carlos Chagas Institute, FIOCRUZ, Curitiba, Paraná, Brazil

Short title: Fungal EVs on communication and immunomodulation

Corresponding author: Fausto Almeida, fbralmeida@usp.br

Keywords: virulence factors, pathogenic fungi, intraspecies, interspecies, immunostimulation, fungal communication

Word count abstract: 194

Word count text: 9.454

bioRxiv preprint doi: https://doi.org/10.1101/2025.02.03.636213; this version posted February 4, 2025. The copyright holder for this preprint (which was not certified by peer review) is the author/funder, who has granted bioRxiv a license to display the preprint in perpetuity. It is made available under a CC-BY-NC-ND 4.0 International license.

Abstract

Extracellular vesicles (EVs) play crucial roles in fungal communication and host immune modulation, representing potential therapeutic targets for fungal infections. This study investigated the role of fungal EVs in both intra- and interspecies communication, focusing on their effects on virulence and immune responses. Co-incubation experiments were performed using EVs derived from *Candida albicans* and *Candida auris* to assess interactions with *C. albicans* planktonic cells and biofilms, as well as *Cryptococcus neoformans* and *Cryptococcus gattii* EVs interacting with *C. neoformans* cultures. EVs were observed associating with recipient cell surfaces, suggesting subsequent internalization. Functional assays revealed that EV exposure led to increased expression of *Cap59, Lac1, Ure1*, and *Erg11* genes, correlating with reduced antifungal susceptibility in both planktonic and biofilm forms. Additionally, EVs facilitated cross-species communication, enhancing biofilm adhesion and dispersion, which underscores their role in phenotypic modulation. Macrophages stimulated with fungal EVs exhibited receptor-specific gene expression changes, notably the upregulation of *galectin-3*, along with a pro-inflammatory phenotype marked by increased *iNOS* expression and elevated cytokine levels (IL-1β, IL-6, and IL-8). Collectively, these findings underscore a critical role for fungal EVs in interspecies communication, biofilm regulation, and immune modulation, offering valuable insights into fungal pathogenicity mechanisms.

Importance

Currently, no vaccines exist to prevent fungal infections, underscoring the need for new therapies. As fungal diseases increase globally, understanding fungal biology is essential to identifying treatment targets. Fungi use EVs to communicate and evade immune responses. EVs mediate cell-cell communication, transporting proteins, polysaccharides, lipids, and nucleic acids – serving as “messages” exchanged within a fungal network. Understanding how these vesicles facilitate communication not only within a single species but also across different fungal species can shed light on their contribution to infection persistence and cross-species adaptability. Moreover, EVs may have a broader role in inter-kingdom communication, influencing how fungi interact with host immune cells. The impact of fungal EVs on human innate immune responses

bioRxiv preprint doi: https://doi.org/10.1101/2025.02.03.636213; this version posted February 4, 2025. The copyright holder for this preprint (which was not certified by peer review) is the author/funder, who has granted bioRxiv a license to display the preprint in perpetuity. It is made available under a CC-BY-NC-ND 4.0 International license.

remains a largely underexplored area, with significant gaps in our knowledge. This study aims to examine how fungal EVs affect immune responses and whether their signaling varies across species, potentially revealing new therapeutic targets.

Introduction

In recent decades, fungi have emerged as significant human pathogens, posing a global threat to human health. This trend highlights the urgent need to address fungal infections, particularly with the rise of multidrug-resistant strains (1). The increase in fungal infections is closely associated with the rising number of immunocompromised individuals, as well as the fungi's own evolving capabilities, such as enhanced pathogenicity and the ability to colonize new ecological niches (2–4). Fungal infections now affect over 1 billion people annually, with 2.55 million deaths reported worldwide, particularly among immunocompromised individuals (2, 5). Despite the considerable global health burden, the U.S. Food and Drug Administration (FDA) has yet to approve any vaccines for fungal infections (6). In 2022, the World Health Organization published its first ever *fungal priority pathogens list*, which categorizes pathogens into critical, high, and moderate threats. Among the "critical importance" group are *Aspergillus fumigatus*, *Candida albicans*, *Candida auris*, and *Cryptococcus neoformans*. These pathogens represent significant challenges due to their virulence and resistance to treatment. (3, 7).

Candida albicans, and more recently *C. auris*, are among the most prevalent *Candida* species associated with candidiasis in humans, causing nosocomial outbreaks with mortality rates exceeding 40% in some studies (1, 8). Effective control strategies, including the use of antifungal therapies and rapid diagnostic tools, are crucial to prevent disease progression. Similarly, cryptococcosis, caused by *C. neoformans* and *C. gattii*, poses a comparable mortality risk due to severe pulmonary and central nervous system infections (1, 9). The ability of both *Candida* and *Cryptococcus* to establish infections is facilitated by several key virulence factors, such as thermotolerance, dimorphism, biofilm formation, capsule production, adhesins, and hydrolytic enzymes, all of which contribute to their pathogenicity and resistance to host defenses (3).

Fungal EVs play a critical role in pathogenesis, often described as "virulence bags" due to their role in transporting a variety of bioactive molecules, including proteins,

bioRxiv preprint doi: https://doi.org/10.1101/2025.02.03.636213; this version posted February 4, 2025. The copyright holder for this preprint (which was not certified by peer review) is the author/funder, who has granted bioRxiv a license to display the preprint in perpetuity. It is made available under a CC-BY-NC-ND 4.0 International license.

lipids, nucleic acids, polysaccharides, toxins, and pigments. These components facilitate fungal dissemination and immune evasion within the host environment (10), functioning as carriers for molecules destined for the extracellular space (11). EVs are spherical structures enclosed by a bilayer membrane, categorized into small (<200 nm) and large (>200 nm) vesicles, following MISEV2023 (*Minimal information for studies of extracellular vesicles*) guidelines (12). Our group has shown that fungal EVs play a key role in facilitating communication among fungal cells within the same species (intraspecies interactions) (13). Additionally, these EVs also act as immunomodulators in host-pathogen interactions, as evidenced by *in vitro* studies involving immune cells (14–17).

Fungi can internalize EVs, triggering a variety of responses, including changes in gene expression. These responses are critical for fungal pathogens, influencing key processes such as antifungal tolerance, virulence, morphogenesis, and growth (13, 18). By coordinating fungal communities, EVs enhance their survival and adaptability within the host environment (19). EVs play a significant role in *C. albicans* biofilm formation and the yeast-to-hypha transition (13, 20, 21). However, further studies are needed to elucidate the roles of EVs in cross-species signaling and their impact on fungal biology during active infections.

Emerging studies are also investigating interactions between different *Candida* species mediated by EVs, prompted by epidemiological data suggesting that multispecies infections are becoming more common (22). In *Cryptococcus* species, EVs regulate key virulence mechanisms and enable long-distance signaling (23), with research on this topic spanning over the past 15 years (24, 25). Beyond their role in cell wall dynamics, cryptococcal EVs are critical for capsule biogenesis and maintenance, as they transport the major capsule component, *glucuronoxylomannan* (GXM), through a trans-cell wall export mechanism (11). Although coinfections involving different *Cryptococcus* species in humans are considered rare (26, 27), studying EV-mediated interspecies communication provides valuable insights into the conservation of cellular communication mechanisms across fungal species.

In addition to their role in cellular communication, EVs are potent stimulators of host immunity (28). Most research on the immunostimulatory effects of fungal EVs has been conducted *in vitro* using immune cells, primarily focusing on species from the *Candida* and *Cryptococcus* genera (28, 29). EVs from *C. albicans* were implicated in

bioRxiv preprint doi: https://doi.org/10.1101/2025.02.03.636213; this version posted February 4, 2025. The copyright holder for this preprint (which was not certified by peer review) is the author/funder, who has granted bioRxiv a license to display the preprint in perpetuity. It is made available under a CC-BY-NC-ND 4.0 International license.

126 modulating both innate and adaptive immune responses, including the induction of
127 nitric oxide (NO) production and the regulation of inflammatory response (30, 31). Key
128 virulence factors in *C. albicans* EVs that contribute to host immune activation include
129 phosphatidylserine, glucosylceramide, and small RNAs (28, 31). In *Cryptococcus*, EVs
130 also carry important virulence factors such as glucosylceramide and small RNAs.
131 However, two other prominent factors, GXM and melanin, are known for their
132 cytotoxic effects and ability to suppress phagocytosis, respectively (28, 32). While some
133 studies report an anti-inflammatory response, characterized by increased IL-10 and
134 TGF-β (Transforming Growth Factor β) in macrophages stimulated with *C. neoformans*
135 EVs (29, 33), other research has observed pro-inflammatory responses following
136 stimulation with EVs from *C. neoformans* and *C. gatti* (32, 34).

137 In this study, we aimed to explore the role of fungal EVs in communication and
138 immune modulation, isolating and characterizing EVs from *C. albicans, C. auris, C.*
139 *neoformans,* and *C. gattii.* We investigated intra- and interspecies communication by
140 assessing EVs uptake and impact on planktonic cells, biofilm formation, antifungal
141 tolerance, and the transfer of capsular material. Additionally, we examined the
142 immunomodulatory activity of these EVs on THP-1 human macrophage-like cells. This
143 analysis focused on internalization, potential cytotoxic effects, the production of pro-
144 and anti-inflammatory cytokines, and the mRNA expression of immune response-
145 associated genes.

146

147 **Results**

148 **Fungal EVs as mediators in intra- and inter-species communication**

149 The detailed characterization of EVs structure, cargo, and biological significance began
150 around 2007 with the study of EVs from *C. neoformans* (29). Understanding the
151 characteristics of EVs may reveal species-specific attributes that are critical for their
152 function. Figure 1 (A-D) presents the results of Nanoparticle Tracking Analysis (NTA)
153 and Transmission Electron Microscopy (TEM) for EVs isolated from cultures of *C.*
154 *albicans* ATCC64548, *C. auris* clinical isolate 470/2015, *C. neoformans* H99, and *C.*
155 *gattii* R265. Characterization of these EVs revealed a heterogeneous population in all
156 samples, ranging from small EVs (sEVs) with a size of < 200 nm to large EVs (lEVs)
157 with > 200 nm (summarized in Fig. 1E). The yield of EVs recovered after the isolation

bioRxiv preprint doi: https://doi.org/10.1101/2025.02.03.636213; this version posted February 4, 2025. The copyright holder for this preprint (which was not certified by peer review) is the author/funder, who has granted bioRxiv a license to display the preprint in perpetuity. It is made available under a CC-BY-NC-ND 4.0 International license.

protocol (centrifugation, filtration, and ultracentrifugation) was quantified by the EV-to-fungal cell ratio, a method suggested for evaluating and comparing EV isolation from solid media-based cultures. Zeta potential, an important indicator of surface charge and stability, was also measured using Dynamic Light Scattering (DLS). The zeta potential of fungal EVs ranged from -8 to -15 mV, indicating a stable colloidal suspension under physiological conditions (Fig. 1F).

Our group previously demonstrated the role of fungal EVs in intraspecies communication (13). In this study, we explore the potential for EVs to serve as vehicles for interspecies communication, focusing on their ability to be "sent" and "received" as messages between fungi of different species. Using labeled EVs and fluorescence microscopy, we observed the recognition and possible internalization of EVs from different species. Specifically, we detected interactions between *C. albicans* cells and *C. auris* EVs, *C. gattii* cells and *C. neoformans* EVs, and an intergeneric interaction between *C. auris* cells and *C. neoformans* EVs (Fig. 2A). Additionally, scanning electron microscopy (SEM) revealed an increase in vesicle-like structures adhered to the surface of recipient cells after incubations with EVs isolated from other species, supporting the hypothesis that EVs interact with the fungal cell wall and/or membranes before internalization (Fig 2B and C).

Extracellular vesicles are frequently referred to as "virulence bags," as they transport proteins and other biomolecules between cells (3). In our study, we explored the biological impact of EVs in interspecies communication, using *C. neoformans* ΔCap67 (an acapsular mutant) as a model to better understand the role of EVs in the transmission of virulence factors. We chose the *C. neoformans* ΔCap67 strain to avoid the capsule when exploring EV delivery, allowing for a more detailed examination of the cell surface without interference from capsular components that could hinder the visualization of EV incorporation. This approach was particularly valuable for investigating the transfer of GXM and other associated molecules from EVs derived from wild-type strains (H99 or R265), to determine whether the transfer of EVs cargo is sufficient to restore the mutant phenotype. While *C. neoformans* var. *grubii* H99 is classified as serotype A, the ΔCap67 mutant is a serotype D strain derived from strain B3501 (*C. neoformans* var. *neoformans*) (35). ΔCap67 is also referred to as strain B4131 in the literature, and, as well as the ΔCap59 strain (an acapsular mutant derived

bioRxiv preprint doi: https://doi.org/10.1101/2025.02.03.636213; this version posted February 4, 2025. The copyright holder for this preprint (which was not certified by peer review) is the author/funder, who has granted bioRxiv a license to display the preprint in perpetuity. It is made available under a CC-BY-NC-ND 4.0 International license.

from H99), its phenotype can be restored by *Cap59* gene complementation (both strains show mutations in *Cap59*) (35, 36).

We firstly examined the effect of adding EVs to planktonic cells to assess their impact on virulence factor expression at the molecular level. Specifically, we selected three genes - *Cap59*, *Lac1*, and *Ure1* – and measured their transcription by qPCR. Our results showed increased expression of these genes when ΔCap67 mutant cells were incubated with EVs from *C. neoformans* and *C. gattii* (Fig. 3A-C). This response was observed in both intra- and interspecies interaction. Even *C. neoformans* ΔCap67 EVs (Fig. S1A – Supplementary Information for *C. neoformans* ΔCap67 NTA data) induced a modest increase in mRNA expression of these genes, albeit at lower levels. Overall, the addition of EVs led to an upregulation of all tested genes, suggesting that EVs directly contribute to the induction of virulence factor production.

Next, we confirmed the presence of GXM in the EVs of *C. neoformans* H99 and *C. gattii* R265, and its absence in *ΔCap67* mutant EVs, using a dot blot assay (Fig. 3D). Co-incubation of EVs from wild-type strains (H99 and R265) with ΔCap67 mutant cells revealed that GXM was incorporated into the mutant's surface, indicating the uptake of a significant amount of the polysaccharide (Fig. 3E). SEM images (Fig. 2C) further demonstrated that the acapsular mutant did not fully acquire a capsular structure after 24 h of co-incubation, in contrast to the complete phenotype reversal seen in the wild-type strain. This was further confirmed by India ink staining, where no significant differences were observed between cells that received EVs and the controls (no EVs added) (Fig. S2 - Supplementary Information).

The characteristics of *C. neoformans* ΔCap67 biofilms were also altered after exposure to EVs. While no significant differences in adhesion were observed when biofilms were incubated with ΔCap67 EVs (compared to biofilms with no EVs added), the highest concentrations of EVs from *C. neoformans* H99 and *C gattii* R265 (10^9 and 10^8 EVs/well, respectively) resulted in a significant increase in the number of adhered cells during the adhesion phase (Fig. 3F-H). The highest concentration of EVs (10^9 EVs/well) was also tested in the biofilm dispersion assay, where it was shown that EVs influence the dispersion phase. However, no statistically significant differences were observed in the levels of dispersion between EVs from the same or different strains (Fig. 3I). Additionally, the impact of EVs on antifungals susceptibility was assessed, revealing that biofilms incubated with EVs from the wild-type strains of *C. neoformans*

bioRxiv preprint doi: https://doi.org/10.1101/2025.02.03.636213; this version posted February 4, 2025. The copyright holder for this preprint (which was not certified by peer review) is the author/funder, who has granted bioRxiv a license to display the preprint in perpetuity. It is made available under a CC-BY-NC-ND 4.0 International license.

and *C. gattii* exhibited increased tolerance to antifungals (Fig. 3J). The effect on virulence factors was further confirmed by a spot test, where planktonic cells co-incubated with EVs from *C. neoformans* and *C. gattii* showed reduced antifungal susceptibility on agar plates containing various concentrations of fluconazole (Fig. 3J and Fig. S3 - Supplementary Information).

The biological impact of fungal EVs on interspecies communication was further demonstrated in both planktonic cells and biofilms of *Candida* yeasts. In planktonic *C. albicans* cells, EVs isolated from both *C. albicans* and *C. auris* induced an increase in mRNA expression of *Erg11*, a gene that is up-regulated in azole-resistant isolates. EVs isolated from *C. auris* cultured in fluconazole-containing plates (see Fig. S1B – Supplementary Information for *C. auris* NTA result) also stimulated elevated *Erg11* expression in planktonic *C. albicans*. Notably, qPCR analysis revealed that the increase in *Erg11* expression was approximately 2-fold higher than that observed with EVs from *C. albicans* or untreated *C. auris* EVs (Fig. 4A). Additionally, spot tests demonstrated a difference in fluconazole susceptibility between planktonic *C. albicans* cells incubated with EVs from *C. auris*, in which at high fluconazole concentrations, *C. albicans* cells exposed to *C. auris* EVs exhibited a more tolerant phenotype (Fig. 4B).

The cross-communication between *C. albicans* and *C. auris* through EVs was evaluated using assays of biofilm adhesion, dispersion, and fluconazole tolerance. As seen in planktonic assays, exposure to EVs also altered azole tolerance in *C. albicans*. In *C. albicans* biofilms, fluconazole treatment resulted in an approximately 62% reduction in cell viability of biofilm mass (control). However, biofilms treated with *C. albicans* EVs showed a reduction of approximately 47%, and those treated with *C. auris* EVs exhibited a reduction of 42%, suggesting a decreased susceptibility to fluconazole in the presence of EVs (Fig. 4C). In biofilms of both *C. albicans* and *C. auris*, fungal cell/EV ratios ranging from 1:10 to 1:1000 (10^7 to 10^9 EVs/well) resulted in significantly increased biofilm adhesion compared to the control (no EVs added). No differences were observed when EV concentrations were < 10^6 EVs/well (Fig. 4D, E, G, H). The EV concentrations that enhanced biofilm adhesion were selected for further investigation of their impact on biofilm dispersion. In these assays, biofilms treated with EVs, whether from *C. albicans* or *C. auris*, showed higher levels of dispersed cells compared to the control (Fig. 4 F and I), indicating that both intraspecies and interspecies communication promoted biofilm dispersal.

bioRxiv preprint doi: https://doi.org/10.1101/2025.02.03.636213; this version posted February 4, 2025. The copyright holder for this preprint (which was not certified by peer review) is the author/funder, who has granted bioRxiv a license to display the preprint in perpetuity. It is made available under a CC-BY-NC-ND 4.0 International license.

Fungal EVs as molecules with immunomodulatory properties – the inter-kingdom communication

One of the critical factors in host-pathogen interactions during infection is communication via EVs (34). Fungal EVs play a pivotal role in fungal pathogenicity, as they transfer virulence factors with immunomodulatory properties. These factors are recognized as pathogen-associated molecular patterns (PAMPs), thereby activating the innate immune response (3, 35). Similar to studies conducted with fungal cells, we labeled fungal EVs with a fluorescent dye to observe their incorporation or internalization by immune system cells – specifically, human macrophage-like cell cultures (THP-1 cells). Through fluorescence microscopy, we detected labeled EVs overlapping with regions where THP-1 cells were located (Fig. 5A), suggesting an association with the macrophage-like cell surface and potential internalization. Since the cytotoxic effects of fungal EVs vary depending on the study and experimental conditions, we further investigated their impact on cellular properties during co-incubation of THP-1 cells with EVs from *Cryptococcus* spp. and *Candida* spp. The assay revealed no significant differences in human macrophage-like cells cultured *in vitro* concerning cell size, viability, or concentration following exposure to fungal EVs (Fig. 5B-D).

The stimulation of THP-1 macrophage-like cells by fungal EVs was analyzed using qPCR, targeting the mRNA transcription of polarization markers, receptors, and proteins involved in immune response pathways associated with combating pathogenic fungi (Fig. 6A-M). All fungal EVs induced an up-regulation of *iNOS* (nitric oxide synthase) and either a basal or downregulated expression of *ARG1* (arginase 1) ($p < 0.05$). This response suggests the polarization of macrophages toward the M1 phenotype.

Candida spp. EVs stimulated human macrophages to upregulate the mRNA expression of *TLR4* and *TLR9*. Among these, only *C. albicans* induced significant levels ($p < 0.05$) of *CLEC7A* expression, while *C. auris* specifically stimulated *TLR2*. In contrast, *Cryptococcus* EVs generally showed either basal mRNA expression (not statistically different) or downregulation of the evaluated receptors. For instance, *CLEC7A* was downregulated in response to EVs from both cryptococcal species, and *TLR9* was downregulated following stimulation with EVs from *C. gattii*. Notably, *TLR2* was the only receptor upregulated by *Cryptococcus* EVs, with its expression significantly

bioRxiv preprint doi: https://doi.org/10.1101/2025.02.03.636213; this version posted February 4, 2025. The copyright holder for this preprint (which was not certified by peer review) is the author/funder, who has granted bioRxiv a license to display the preprint in perpetuity. It is made available under a CC-BY-NC-ND 4.0 International license.

289 enhanced in response to *C. neoformans* EVs. Additionally, *LGALS3*, the gene encoding
290 galectin-3 – a protein that binds beta-galactosides and exhibits antimicrobial activity –
291 was consistently up-regulated in THP-1 cells across all EVs tested.

292 The immunomodulatory effects of fungal EVs exhibited pattern of *STING*
293 downregulation. Specifically, *Candida* EVs downregulated *SYK* expression, while
294 *Cryptococcus* EVs let to the expression of *CGAS*. Regarding *CARD9*, EVs from *C.*
295 *neoformans* caused a significant downregulation of its expression, whereas incubation
296 with *C. albicans* EVs resulted in increased mRNA expression in THP-1 cell cultures.
297 *MYD88*, a gene encoding an adapter protein widely studied in immune responses, was
298 upregulated in response to all fungal EV stimuli, with the most pronounced effects
299 observed for EVs derived from *C. auris* and *C. neoformans*.

300 The quantification of pro- and anti-inflammatory cytokines in the supernatant of
301 macrophage cultures performed by ELISA, allowed the characterization of the immune
302 response profile mediated in THP-1 cells stimulated by fungal EVs. Pro-inflammatory
303 cytokines IL-1β, IL-6, and IL-8 were produced at significantly higher levels compared
304 to the control (non-stimulated cells, medium only) when fungal EVs were present in the
305 medium. However, TNF-α levels, while higher than the negative control, were lower
306 compared to the other pro-inflammatory cytokines (Fig. 7A, C, D, F). Analyzing the
307 response by fungal genera, THP-1 cells stimulated with *C. albicans* EVs produced more
308 IL-6 than those stimulated with *C. auris* EVs, whereas *C. auris* EVs induced higher
309 levels of IL-1β and TNF-α. In the *Cryptococcus* group, EVs from *C. neoformans*
310 stimulated higher levels of IL-1β and IL-8 compared to EVs from *C. gatti*. Regarding
311 the anti-inflammatory cytokines, IL-4 levels remained below the control for all EV
312 stimuli, with very low concentrations being detected. Conversely, IL-10 was produced
313 at levels significantly higher than in control cells (Fig. 7B, E). Taken together, these
314 findings suggest a predominance of a pro-inflammatory response mediated by THP-1
315 cells in the presence of fungal EVs.

316

317 **Discussion**

318 *Cross-talk* can be defined as an exchange of signals between communicating organisms
319 even over a distance, functioning as a shared “language” based on extracellular signals.
320 These signals are interpreted to coordinate critical processes, such as the survival of

bioRxiv preprint doi: https://doi.org/10.1101/2025.02.03.636213; this version posted February 4, 2025. The copyright holder for this preprint (which was not certified by peer review) is the author/funder, who has granted bioRxiv a license to display the preprint in perpetuity. It is made available under a CC-BY-NC-ND 4.0 International license.

pathogenic fungi during infection establishment (37). In fungal communication, essential biological functions are influenced by the exchange of these "messages", including mating, growth, morphological transitions, and virulence (38). Cross-talk in fungi is partially mediated by EVs - nano-sized structures with bilayer membranes that carry proteins, lipids, glycans, pigments, and nucleic acids (11). Our group recently demonstrated the role of EVs from human pathogenic fungi in intraspecies cellular communication, revealing at the molecular level their impact on gene expression and fungal proliferation control (13). However, this fungal network coordination mechanism does not appear to be limited to the same fungal strain or species. Although still an emerging field, growing evidence supports the existence of EV-mediated interspecies communication, showing significant biological effects, such as biofilm formation and drug-resistance phenotypes, following cross-species interaction (22).

Extracellular vesicles were successfully isolated from cultures of *C. albicans*, *C. auris*, *C. neoformans*, and *C. gattii* using the protocol described in Reis et al. (2019) (39). The structure and size of fungal EVs were confirmed through NTA and TEM, corroborating findings from several studies (39–42). These studies consistently described fungal EVs as a heterogeneous population of round-shaped structures, predominantly around 200 nm in size. Regarding the EV-to-cell ratio, our findings align with observations from other research groups (43), which reported up to 10 EVs per cell in similar isolation protocols.

Zeta potential, a measure of particle surface charge, is a key determinant in the stability and functionality of EVs (44). Under physiological conditions, negatively charged particles, including fungal EVs, exhibit enhanced internalization by phagocytic cells such as macrophages, while positively charged particle tend to be preferentially internalized by non-phagocytic cells (44, 45). In this study, fungal EVs consistently exhibited negative zeta potential values, indicating stable colloidal suspensions with reduced likelihood of aggregation. This characteristic support their stability in extracellular environments and suggest increased recognition and uptake by innate immune cells. Similar findings in nanoparticle systems have shown that negative zeta potential reduces protein corona formation, prolongs circulation time, and improves delivery efficiency to target tissues (46). The stability and charge properties of EVs may be leveraged for therapeutic delivery, enhancing biodistribution and targeting infected or inflamed tissues with elevated phagocytic activity (47). This preferential interaction

bioRxiv preprint doi: https://doi.org/10.1101/2025.02.03.636213; this version posted February 4, 2025. The copyright holder for this preprint (which was not certified by peer review) is the author/funder, who has granted bioRxiv a license to display the preprint in perpetuity. It is made available under a CC-BY-NC-ND 4.0 International license.

could be further exploited by engineering fungal EVs to carry antifungal compounds or immune modulators, optimizing their delivery to target sites.

It has been demonstrated that vesicular transport in fungi occurs bidirectionally across the fungal cell wall, allowing the export of EVs to the external environment as well as the internalization into intracellular compartments after binding to fungal surface receptors (18, 19). Some studies suggest key processes that may be necessary for EV uptake, including the passage of EVs through cell wall pores approximately 5 nm in size (or up to 400 nm under stress conditions), enzymatic modifications of the cell wall (mediated by enzymes carried by EVs), and transit through specific cellular channels (18, 48). Our group previously reported the uptake and association of radiolabeled EVs by cells of different fungal species, such as *C. albicans*, *Paracoccidioides brasiliensis*, and *A. fumigatus* (13). In the present study, we demonstrate similar events in *C. albicans*, *C. auris*, *C. neoformans*, and *C. gattii* using a fluorescent lipophilic membrane stain. Additionally, SEM revealed an increase in vesicle-like structures on fungal cell surfaces. Despite these findings, the internalization of EVs by fungal cells remains an emerging field that requires further investigation to fully elucidate and consolidate our understanding of these mechanisms.

After the EV uptake, fungal cells can be triggered to mount specific responses mediated by molecules transported within these vesicles. For instance, polysaccharides like GXM found in *Cryptococcus* EVs can be assimilated by receptor cells and subsequently decorate their surface (49). Since the vesicle cargo includes polysaccharides, proteins, RNA, DNA, and other bioactive molecules, it is expected that recipient cells respond to their release within the intracellular environment. Our results revealed an increase in the mRNA expression of genes associated with virulence following co-incubation with EVs derived from the same or different fungal species. Among these genes, *Lac1* encodes laccase, an enzyme directly involved in melanin production by *Cryptococcus* spp. (50); *Ure1* encodes urease, an enzyme responsible for the hydrolysis of urea into ammonia and carbamate (51); and *Erg11* encodes sterol 14-demethylase, a key enzyme in ergosterol biosynthesis (52). The mRNA expression of all these genes was significantly altered after the addition of EVs to fungal cultures. However, further studies are needed to clarify whether the observed increase in mRNA expression is directly caused by mRNA molecules transported within EVs or if it results from other expression-activating mechanisms.

bioRxiv preprint doi: https://doi.org/10.1101/2025.02.03.636213; this version posted February 4, 2025. The copyright holder for this preprint (which was not certified by peer review) is the author/funder, who has granted bioRxiv a license to display the preprint in perpetuity. It is made available under a CC-BY-NC-ND 4.0 International license.

Cap59 is a gene essential for capsule formation, as its absence or mutation results acapsular mutants (53). In our study, an increase in *Cap59* mRNA expression was conserved in cultures of ΔCap67 mutants exposed to EVs. However, TEM and India Ink staining did not reveal a restoration of the wild-type capsule phenotype. We propose two possible explanations for the reaction observed in the dot blot analysis: (a) GXM polysaccharides from EVs are being recognized as annexed structures on the cell surface and/or (b) a thin and irregularly spaced GXM layer might be produced by the acapsular mutant through the translation of *Cap59* mRNA (originating from the wild-type strain and free from missense mutations). A similar outcome was reported by Bielska et al. (2018) (23), who demonstrated that EVs from the wild-type *C. gattii* R265 strain were insufficient to restore capsule formation in an acapsular mutant (R265ΔCap10). Therefore, even though increased *Cap59* mRNA expression was detected by qPCR, this may reflect an upregulated expression of the mutated gene sequence, which would not translate into effective capsule formation.

Beyond planktonic cells, EVs can also influence fungal biofilms. Biofilm formation in fungi is a multi-stage process that includes adhesion, growth, maturation, and dispersion phases (54). Adhesion is a critical initial step, as fungal pathogens rely on this process to colonize host tissues and initiate infection. Adhesins and their corresponding host cell ligands play a pivotal role in biofilm formation (55). Research on the effects of EVs on biofilms, particularly during the adhesion phase, is still emerging. To the best of our knowledge, our study is one of the first to investigate the effects of interspecies communication in biofilm formation. While Zarnowski et al. (2022) (56) explored intra- and interspecies communication in *Candida* spp. and observed predominant antagonistic interactions between EVs from one species and biofilms from another, our findings suggest a different interaction pattern between EVs and the biofilms of *C. albicans* and *C. auris.* To address this question, we conducted experiments across a broad range of EV concentrations. Our results indicate that the concentration of EVs is a determining factor for their biological effects, whether enhancing or inhibiting biofilm adhesion, in both *Candida* and *Cryptococcus* species. Notably, EVs derived from *C. neoformans* ΔCap67 mutants did not enhance biofilm adhesion. We hypothesized that this occurs because GXM polysaccharide, which are transported by EVs from the wild-type strains, are essential for increasing adhesion levels. The absence of GXM in ΔCap67 mutants is a well-known limiting factor for biofilm formation (57).

bioRxiv preprint doi: https://doi.org/10.1101/2025.02.03.636213; this version posted February 4, 2025. The copyright holder for this preprint (which was not certified by peer review) is the author/funder, who has granted bioRxiv a license to display the preprint in perpetuity. It is made available under a CC-BY-NC-ND 4.0 International license.

Dispersion represents the final stage of the biofilm lifecycle, characterized by the detachment and release of cells – primarily in the yeast form - from the biofilm to colonize new surfaces (58). This process is tightly regulated by various molecules and environmental factors, including pH, nutrient availability, and other external cues. Recently, EVs are suggested as key regulators of biofilm formation and detachment (59). Previous studies using exogenous EV add-back assays in both intra- and interspecies contexts (21, 22, 58) have demonstrated that EV administration can significantly impact dispersion levels. Our findings align with these observations, showing that EVs modulated biofilm dispersion different fungal species. Interestingly, our results suggest that EVs may carry a conserved set of core effectors capable of triggering similar responses in fungi of other species. However, the biological responses elicited by EVs are not universally identical across species. Variations in response appear to correlate with the phylogenetic distance between the EV donor and recipient species, indicating that EV-mediated communication does not convey a universally consistent signal within a fungal genus (22).

In *Candida* spp., studies have linked the functional cargo transported by EVs to increased protection against antifungal treatment when EVs are added to susceptible strains (21, 22). Specifically, reduced susceptibility to fluconazole and caspofungin in *C. albicans* biofilms supplemented with EVs has been attributed to their positive role in enhancing the extracellular matrix architecture (58–60). In our study, we observed differences in antifungal tolerance between planktonic and biofilms of *C. albicans* and *C. neoformans* ΔCap67, corroborating findings from previous studies that reported a similar role for fungal EVs in both intra- and interspecies interactions (22, 40). Chan et al. (2022) (40) identified modulation of antifungal tolerance - specifically against Amphotericin B – only in interactions between fungi and EVs from the same species (*C. auris*). However, our results revealed that this modulation can also occur at the interspecies level (*C. albicans* x *C. auris*) in experiments using fluconazole. The upregulation of *Erg11* expression observed in planktonic *C. albicans* exposed to EVs, suggests that increased ergosterol synthesis could be a plausible explanation for the enhanced resistance to azoles via EV-mediated communication. Data regarding changes in antifungal tolerance following EV exposure in *Cryptococcus* spp. or other fungal pathogens, particularly in cross-species interactions, remain limited in the literature and warrant further investigation.

bioRxiv preprint doi: https://doi.org/10.1101/2025.02.03.636213; this version posted February 4, 2025. The copyright holder for this preprint (which was not certified by peer review) is the author/funder, who has granted bioRxiv a license to display the preprint in perpetuity. It is made available under a CC-BY-NC-ND 4.0 International license.

Candida spp. and *Cryptococcus* spp. are fungi belonging to distinct taxonomic classes, *Ascomycota* and *Basidiomycota*, respectively, which are phylogenetically distant (2). While *Cryptococcus* species, *Candida albicans*, and *Candida auris* are not expected to share the same ecological niches, they were utilized in this proof-of-concept study to demonstrate the principle of interspecies communication using three medically significant fungal species. Despite their genotypic and phenotypic differences, this study revealed that interspecies communication mediated by EVs can occur between evolutionary divergent fungi, resulting in biologically relevant effects on recipient cells.

Pathogenic fungal cells communicate with each other (pathogen-to-pathogen), forming a network during infection to coordinate actions through the transport of virulence factors and other molecules. They also communicate with host cells (pathogen-to-host), establishing an inter-kingdom interaction that modulates the host immune response (61). Previous studies, including work from our group, have shown that EVs from *Candida haemulonii*, *C. albicans*, and *C. neoformans* do not exhibit cytotoxic effects on macrophages. Despite this, immune cells remained capable of responding to EV stimuli through the production of cytokines, antibodies, and antimicrobial compounds, among others defense mechanisms (16, 61). Additionally, some researchers have suggested a correlation between EV size and cytotoxicity, with small EVs (sEVs) being less cytotoxic than large (lEVs) (45). Understanding the internalization of fungal EVs by innate immune cells is a rapidly evolving field. In our study, we contributed to this growing body of knowledge by demonstrating the ability of human macrophages to internalize and elicit specific responses against EVs derived from four different species of pathogenic fungi. Furthermore, our findings indicate low or absent cytotoxicity of the tested fungal EVs. This was supported by the lack of significant statistical differences in macrophage viability and cellular properties when comparing treated and untreated groups.

Pathogens invade the host and release EVs to facilitate communication between pathogenic cells, exchanging “messages” about the local environment. These messages can be intercepted by immune system cells, triggering a response against the intruder (62). The stimulation of macrophages by fungal EVs can affect cellular signaling pathways in diverse ways. This process begins with recognition by pattern recognition receptors (PRRs) and may culminate, for example, in the induction of macrophage polarization into M1 (classically activated) or M2 (alternatively activated) phenotypes

bioRxiv preprint doi: https://doi.org/10.1101/2025.02.03.636213; this version posted February 4, 2025. The copyright holder for this preprint (which was not certified by peer review) is the author/funder, who has granted bioRxiv a license to display the preprint in perpetuity. It is made available under a CC-BY-NC-ND 4.0 International license.

(63). M1-polarized macrophages are characterized by the release of high levels of pro-inflammatory cytokines, such as IL-1β, IL-6, TNF-α, and IFNγ, and exhibit potent intracellular pathogen-killing activity mediated by inducible nitric oxide synthase (*iNOS*) and reactive oxygen species (ROS) (64). In contrast, M2 macrophages can be marked by the expression of arginase 1 (*ARG1*) and produce significant levels of anti-inflammatory, such as IL-10 and TGF-β. These cells are primarily involved in tissue repair, remodeling, and suppression of the immune response (64, 65). Arginase 1 competes with nitric oxide synthase for the substrate L-arginine, converting it into urea and ornithine. This effect contrasts with *iNOS*, which converts L-arginine into citrulline and nitric oxide (NO) (66).

Our results suggest that THP-1 macrophage-like cells were polarized toward the M1 phenotype following stimulation with fungal EVs. This pro-inflammatory behavior has also been reported for EVs from *Candida* spp. (30, 44, 67), *Cryptococcus* spp. (34), and other fungi such as *Aspergillus flavus, A. fumigatus, P. brasiliensis,* and *Tricophyton interdigitale,* among others (14, 15, 17, 68). Oliveira et al. (2010) associated stimulation of immune cells with *C. neoformans* EVs to an anti-inflammatory response. However, our findings revealed the opposite effect, a discrepancy that may be attributed to differences in the cytokines evaluated and experimental conditions. As highlighted by Brandt et al. (2024), the effects of *C. neoformans* EVs on immune cell interactions remain underexplored, underscoring a significant research gap that warrants further investigation.

While fungal recognition by immune system cells is a well-explored topic, the recognition of EVs remains underexplored. In line with observations by Honorato et al. (2024) (69), we also detected enhanced expression of *TLR4* following stimulation with *C. albicans* EVs, as well as *C. auris* EVs. This response may be linked to EV surface decorations, including *O*- and *N*- linked mannans, chitin-related structures, and β-1,3 glucans (69). TLR2 and Dectin-1 have been suggested as key receptors involved in fungal EV recognition (17, 70, 71). In our study, we observed species-specific variations in receptor expression: Dectin-1 (*CLEC7A)* was upregulated by *C. albicans* EVs, while *TLR2* was upregulated by *C. auris* and *C. neoformans* EVs. *MYD88* activation is a downstream process event in the TLR2 and TLR4 (61) signaling pathways, aligning with our findings. The detection of distinct receptor activation (or inhibition) profiles may stem from structural differences in EVs or reflect species- and

bioRxiv preprint doi: https://doi.org/10.1101/2025.02.03.636213; this version posted February 4, 2025. The copyright holder for this preprint (which was not certified by peer review) is the author/funder, who has granted bioRxiv a license to display the preprint in perpetuity. It is made available under a CC-BY-NC-ND 4.0 International license.

519 strain-specific strategies employed by pathogenic fungi to evade the immune responses
520 (61, 70). The expression of *TLR9* was a particularly noteworthy finding in our study for
521 two reasons: (1) EVs from both *Candida* spp. significantly upregulated *TLR9*, and (2)
522 *C. gattii* EVs significantly downregulated *TLR9*. Based on Brown et al. (2024) (3) and
523 Vargas et al. (2020) (72), we hypothesize that the enhanced expression of *TLR9* in
524 response to *Candida* spp. EVs may be associated with chitin and nucleic acids present
525 in these vesicles. Conversely, the downregulation of *TLR9* by *C. gatti* EVs may
526 represent an immune evasion strategy, as TLR9-mediated signaling cascades are crucial
527 for host resistance against *C. gatti* infections (73).

528 The immunomodulatory role of Galectin-3 has previously been described in the control
529 of *C. neoformans* and *P. brasiliensis* infections, where its upregulation was observed in
530 infected animals. This lectin was shown to impact EV disruption, inhibit fungal growth,
531 and enhance EV uptake by macrophages (74, 75). Our results revealed an increased
532 expression of *LGALS3* when THP-1 cells were stimulated with fungal EVs, suggesting
533 the involvement of this lectin not only in the recognition and destabilization of *C.*
534 *neoformans* EVs but also in EVs derived from *C. albicans*, *C. auris*, and *C. gattii*. The
535 recognition of *Candida* species by immune cells is typically associated with the Dectin-
536 1 receptor and mediation through the Syk/CARD9 signaling pathway, where Syk
537 appears to play a more direct role in antifungal immunity than CARD9 (76). However,
538 it is also possible to observe a CARD9-dependent but Syk-independent response during
539 *C. albicans* recognition. This mechanism involves the intracellular receptor NOD2
540 (*Nucleotide-binding oligomerization domain* 2) (76, 77), which may partially explain
541 the observed increase in *CLEC7A* and *CARD9* expression alongside reduced *SYK*
542 expression in macrophages stimulated by *C. albicans* EVs.

543 The contribution of STING (*Stimulator of Interferon Genes*) during fungal infections
544 remains under discussion, as its activation has been shown to play a negative
545 modulatory role in antifungal immunity following recognition of fungal EVs (78–80).
546 Harding et al. (80) used *C. albicans* EVs to stimulate bone marrow-derived
547 macrophages for 6 hours, observing activation of the cGAS (*cyclic GMP-AMP*
548 *synthase*)-STING pathway. However, our results demonstrated *STING* mRNA
549 downregulation in macrophages stimulated with all fungal EVs tested. We propose that
550 this discrepancy may stem from several factors, including differences in fungal strains,
551 vesicle cargo composition (which depends on fungal culture conditions), cell lineages,

bioRxiv preprint doi: https://doi.org/10.1101/2025.02.03.636213; this version posted February 4, 2025. The copyright holder for this preprint (which was not certified by peer review) is the author/funder, who has granted bioRxiv a license to display the preprint in perpetuity. It is made available under a CC-BY-NC-ND 4.0 International license.

552 macrophage stimulation duration (6 h vs. 20 h), immunomodulatory effects of fungal
553 EVs, or even a macrophages strategy to mitigate excessive STING activation, which
554 could be detrimental to immune cells. In summary, immune responses and activated
555 pathways are both fungal- and EV composition-dependent (81). In addition to STING,
556 CGAS is another key component of this pathway. Its downregulation has been linked to
557 increased levels of pro-inflammatory cytokines (*IL-1β, IL-6*, and *TNF-α*) in the context
558 of *A. fumigatus* infections (82). Following THP-1 stimulation with EVs, *C. neoformans*
559 – and especially *C. gattii* - EVs induced *CGAS* downregulation. This suppression
560 mechanism may negatively impact the immune response, facilitating fungal immune
561 evasion, as suggested by Peng et al. (2023) and Gu et al. (2023) (78, 82).

562 The characterization of immune response following exposure of host innate immune
563 cells to fungal EVs has advanced through cytokine secretion analysis, enabling the
564 identification of patterns suggestive of pro- or anti-inflammatory responses (62). EVs
565 from *C. neoformans*, *C. gattii*, *C. albicans*, and *C. auris* were previously described as to
566 elicit pro-inflammatory effects in immune cells (32). These responses typically involved
567 increased production of TNFα, IL-6, IL-8, and IL-12, alongside reduced or less
568 pronounced production of TGF-β and IL-10 (61). Consistent with previously published
569 data on fungal EV immunomodulation, our results indicated a predominance of pro-
570 inflammatory cytokines (IL-1β, IL-6, IL-8, and TNFα) in EV-treated macrophages,
571 accompanied by reduced IL-4 levels. Similarly, decreased anti-inflammatory cytokine
572 production compared to non-treated macrophages has been reported in other studies (44,
573 67, 83). Despite the overall pro-inflammatory profile, IL-10 secretion was observed at
574 lower levels. A pro-inflammatory response following EV recognition may represent a
575 preparatory mechanism to combat fungal infections (62). This inter-kingdom cross-
576 communication between host defense mechanisms and pathogenic fungi highlights a
577 crucial area for further exploration, potentially guiding novel interventions for patients
578 affected by invasive fungal infections (84).

579 Taken together, the results obtained in this study represent valuable tools for the
580 development of antifungal therapies. We demonstrated that fungal cells can
581 communicate with each other via signals carried by EVs, which are interpreted by
582 receptor cells from the same or different species. Although the fungal species studied
583 here are unlikely to be found together in the environment or during infection, they
584 belong to fungal genus that include major human pathogenic fungi as thus serve as

bioRxiv preprint doi: https://doi.org/10.1101/2025.02.03.636213; this version posted February 4, 2025. The copyright holder for this preprint (which was not certified by peer review) is the author/funder, who has granted bioRxiv a license to display the preprint in perpetuity. It is made available under a CC-BY-NC-ND 4.0 International license.

585 representative examples to explore EV-mediated interspecies communication. Using *C.*
586 *albicans*, *C. auris*, *C. neoformans*, and *C. gattii*, as models pathogenic fungi, along with
587 their respective EVs, we showed that these molecular messages can also be directed to
588 or intercepted by immune system cells, exerting significant effects on various targets of
589 the innate immune response. Therefore, investigating fungal EVs offers critical insights
590 into fungal communication network, highlighting the need for further evidence to fully
591 "decode" the mechanisms underlying fungal orchestration during infections.

592

593 **Materials and methods**

594 **Strains and culture conditions**

595 *Candida albicans* ATCC 64548 and a clinical isolate of *Candida auris* 470/2015 (clade
596 IV) were cultured in Sabouraud liquid or solid medium (2% w/v agar) at 37 °C for 48 h,
597 with or without shacking at 200 rpm. *Cryptococcus neoformans* var. *grubii* H99,
598 *Cryptococccocus gattii* R265 (kindly supplied by Prof. Dr. Thiago Aparecido da Silva,
599 UNESP), and the *Cryptococcus neoformans* var. *neoformans* Cap67 mutant (ΔCap67)
600 were cultured in a chemically defined minimal medium containing 15 mM dextrose, 10
601 mM $MgSO_4$, 29.4 mM KH_2PO_4, 13 mM glycine, and 3 μM thiamine. These cultures
602 were incubated under the same conditions described above, as minimal media are
603 associated with increased EVs production (85). The ΔCap67 mutant carries a missense
604 mutation in the *Cap59* gene (position 1345), resulting in an amino acid substitution
605 from glycine (Gly) to serine (Ser). This mutation eliminates capsule formation, resulting
606 in an acapsular strain (Cap^- phenotype) (36, 53).

607 The human monocytic cell line THP-1 (ATCC TIB202) was cultured in RPMI 1640
608 medium (Gibco®) supplemented with 10% (v/v) exosome-depleted fetal bovine serum
609 (FBS) (Vitrocell®), sodium bicarbonate, and penicillin/streptomycin (1000 IU). Cells
610 were maintained in a humidified incubator at 37 °C with 5% CO_2. Differentiation of
611 THP-1 monocytes into adherent macrophage-like cells was induced by treating the
612 cultures with 10 ng/mL Phorbol 12-myristate 12-acetate (PMA) for 24 h.

613

614 **Isolation of EVs**

bioRxiv preprint doi: https://doi.org/10.1101/2025.02.03.636213; this version posted February 4, 2025. The copyright holder for this preprint (which was not certified by peer review) is the author/funder, who has granted bioRxiv a license to display the preprint in perpetuity. It is made available under a CC-BY-NC-ND 4.0 International license.

EVs from all yeasts strains used in this study were isolated following the protocol described by Reis et al. (2019) (39). Briefly, overnight cultures of each yeast strain in 10 mL of Sabouraud medium were counted using a Neubauer chamber. A total of 3,5 × 10^7 cells were inoculated onto each 2% agar Sabouraud plate, with 10 plates per strain used to ensure sufficient EV yield. After 48 h of incubation at 37 °C, yeast material was recovered from the plates using Phosphate-Buffered Saline (PBS). The eluate was centrifuged in a Sorvall LEGEND RT+ (Thermo®) centrifuge at 5,000 × *g* for 15 min to remove larger debris. The resulting supernatant was further centrifuged at 15,000 × *g* for 15 min to eliminate residual cellular material, and the pelleted cells were counted to determine the EV-to-cell ratio. The supernatant was passed through 0.45 µM membrane filters (CORNING®) to remove any remaining debris. Finally, EVs were pelleted by ultracentrifugation at 100,000 × *g* for 1 h at 4 °C using an Optima MAX-XP ultracentrifuge (Beckman®). The EV-enriched pellet was resuspended in ultrapure water (Sigma-Aldrich®) and stored at – 80°C. Subsequent EV analyses were performed in accordance with the MISEV 2023 guidelines (*Mininal Information for Studies of Extracellular Vesicles*) (12).

Nanoparticle tracking analysis (NTA)

Nanoparticle tracking analysis was conducted to characterize the size distribution and quantify fungal EVs. Analysis was performed on a Nanosight NS300 (Malvern®) equipped with NTA 3.0 software, following the manufacturer's instructions. Samples were diluted at a 1:100 ratio in PBS and carefully loaded into the Nanosight system. System parameters were adjusted to detect 20–100 particles per frame, with camera sensitivity set to 14 or above (16). Results of NTA were plotted using OriginPro® 2024 software (OriginLab ©).

Zeta potential

The zeta potential of fungal EVs was measured to evaluate surface charge and colloidal stability, using laser scattering with a Zetasizer Nano ZS (Malvern®) (λ = 580 nm, scattering angle 172°), equipped with Zetasizer software v. 7.1 (Malvern®). Measurements were performed at 25 ºC in a disposable DTS1070 cuvette using PBS as

bioRxiv preprint doi: https://doi.org/10.1101/2025.02.03.636213; this version posted February 4, 2025. The copyright holder for this preprint (which was not certified by peer review) is the author/funder, who has granted bioRxiv a license to display the preprint in perpetuity. It is made available under a CC-BY-NC-ND 4.0 International license.

the dispersant (pH 7.4). Electrophoretic mobility values were converted to zeta potential using the Smoluchowski equation, and each sample was analyzed in triplicate with 10–100 runs per measurement.

Transmission Electron Microscopy (TEM)

Fungal EV samples (1×10^9 EVs) were fixed in a solution containing 2% glutaraldehyde and 2% paraformaldehyde in 0.1 M sodium cacodylate buffer (pH 7.4) for 4 h at 4 ºC. Following fixation, samples were ultracentrifuged at 100.000 × g at 4 ºC for 1 h, and the resulting pellets were resuspended in 200 µL of sodium cacodylate buffer. EV structures were visualized using a JEM 100CXII transmission electron microscope (JEOL®), and images were acquired with a Hamamatsu ORCA-HR digital camera (JEOL®).

Internalization of EVs by fungal cells and human macrophages

The recognition and internalization of EVs secreted by either the same or different fungal species were analyzed using fluorescence microscopy. A volume corresponding to 1×10^9 EVs was stained with 1 uL of Vybrant Dil Cell-Labeling Solution (5 µM, Invitrogen®), a lipophilic fluorescent dye for membrane labeling, and incubated for 20 min at 37 °C. After staining, excess dye was removed by washing with PBS. The samples were subsequently ultracentrifuged at 100.000 × *g* at 4 °C for 1 h, and the resulting EV pellet was resuspended in Sabouraud liquid medium, previously inoculated with fungal cells at a 1000:1 EV-to-fungus ratio, and incubated under agitation at 200 rpm.

Scanning Electron Microscopy (SEM)

Scanning electron microscopy was employed to visualize fungal cell morphology following incubation of *C. albicans* and *C. neoformans* (ΔCap67 mutant) with EVs in Sabouraud medium at a concentration of 1×10^9 EVs and 1×10^6 cells (1000:1 EV-to-fungus ratio) under the following conditions: a) *C. albicans* with EVs from *C. auris*, and b) *C. neoformans* ΔCap67 with EVs from *C. gattii*. Incubation was performed at 37 ºC

bioRxiv preprint doi: https://doi.org/10.1101/2025.02.03.636213; this version posted February 4, 2025. The copyright holder for this preprint (which was not certified by peer review) is the author/funder, who has granted bioRxiv a license to display the preprint in perpetuity. It is made available under a CC-BY-NC-ND 4.0 International license.

with agitation at 200 rpm over 24 h. After incubation, fungal cells were centrifuged at 5,000 × g for 15 min and washed with PBS to remove unbound EVs. Cells were then fixed with 2% paraformaldehyde diluted in PBS for 2 h at 4 ºC, centrifuged again as previously described, and resuspended in a buffer containing 1% osmium tetroxide (OsO_4). Samples underwent dehydrated through a graded ethanol series, followed by critical point drying using an Autosamdri-810 system (Tousimis®). Dried samples were mounted on aluminum stubs with silver paint and coated with gold using a Sputter Coater SCD 050 (Bal-Tec). Finally, the prepared samples were visualized using a JSM-6610 LV scanning electron microscope (JEOL®).

Dot blot

The transfer of virulence factors via EVs was investigated by evaluating the transmission of GXM, the primary component of the cryptococcal capsule, to a non-capsular mutant strain of *C. neoformans* (ΔCap67). A straightforward and effective assay was employed, wherein *C. neoformans* ΔCap67 was incubated with EVs from *C. neoformans* and *C. gattii*. In this assay, *C. neoformans* ΔCap67 cells (1×10^6/mL) were incubated with EVs (1×10^9/mL) derived from *C. neoformans* and *C. gattii* in Sabouraud medium for 24 h at 37 °C with 5% CO_2. After incubation, the cells were harvested by centrifugation at 8.000 × *g* for 15 min, washed with PBS, and 10 µL of each sample were applied to a Polyvinylidene difluoride (PVDF) membrane pre-treated with methanol for 5 min. The membrane was subsequently blocked with 5% (w/v) skim milk in PBS for 30 min and washed three times with PBS-T (PBS + 0.05% Tween 20). Next, the membrane was incubated with the monoclonal antibody 18b7, which specifically binds to GXM (generously provided by Prof. Dr. Anamélia Bocca from FIOCRUZ), for 1 h. Following another washing step, an anti-mouse HRP-conjugated secondary antibody (Sigma®) was applied for 1 h. After five additional washes with PBS, the membrane was treated with a detection solution (Vector Laboratories®), resulting in a visible signal indicating the presence of GXM in the samples.

Co-incubation of *C. albicans* and acapsular *C. neoformans* planktonic cells with EVs

bioRxiv preprint doi: https://doi.org/10.1101/2025.02.03.636213; this version posted February 4, 2025. The copyright holder for this preprint (which was not certified by peer review) is the author/funder, who has granted bioRxiv a license to display the preprint in perpetuity. It is made available under a CC-BY-NC-ND 4.0 International license.

C. neoformans ΔCap67 were grown to the stationary phase in Sabouraud broth. A volume corresponding to 5×10^6 cells from the previous culture was inoculated into 5 mL of fresh Sabouraud broth and mixed with 1×10^9 EVs (1:200 cell/EV ratio) isolated from *C. neoformans* H99, *C. gattii* R265, or self-derived EVs from ΔCap67. Fungal EVs were added at the start of the experiment (0 h) and again after 6 h of incubation. The experiment was conducted over 24 h at 37 °C with shaking at 200 rpm. At designated time points, samples were collected, and India ink staining was performed to visualize potential capsule formation on the cellular surface. Cells were then separated from the culture medium by centrifugation at 8.000 × *g* for 15 min at 4 °C and subjected to RNA extraction using the Quick-RNA Fungal/Bacterial Miniprep kit (Zymo Research®). The isolated RNA was quantified using a NanoDrop One spectrophotometer (Thermo®) and subsequently used to evaluate the expression levels of *Lac1*, *Ure1*, and *Cap59* by qPCR, with results compared to the control culture (*C. neoformans* ΔCap67 without EVs addition).

The effect of fungal EVs on planktonic cells of *Candida* was investigated using a similar experimental design. Cultures of *C. albicans* were first grown to the stationary phase in Sabouraud broth. The same broth volume, cell/EV ratio, and incubation conditions previously described were applied. In this assay, EVs isolated from *C. albicans* and *C. auris* were analyzed. Additionally, EVs from *C. auris* cultured in the presence of fluconazole were included for comparison. After incubation, the cell pellet was collected by centrifugation, and total RNA was purified and quantified as described before for the *C. neoformans* ΔCap67 experiment. The expression level of *Erg11* was then evaluated by qPCR and compared to a control culture (*C. albicans* without EV treatment).

Spot test

The effect of GXM-transmitting EVs on *C. neoformans* ΔCap67 cells was further investigated using a spot assay to assess potential differences in antifungal tolerance. In this assay, 100 µL of EVs (1×10^{10} EVs/mL) derived from *C. neoformans* or *C. gattii* were added to cultures of *C. neoformans* ΔCap67 (1×10^6 cells/mL) in 10 mL of Sabouraud broth. The cultures were then incubated at 37 ºC with shaking at 200 rpm for 24 h. Untreated *C. neoformans* ΔCap67 cultures served as controls. Following

bioRxiv preprint doi: https://doi.org/10.1101/2025.02.03.636213; this version posted February 4, 2025. The copyright holder for this preprint (which was not certified by peer review) is the author/funder, who has granted bioRxiv a license to display the preprint in perpetuity. It is made available under a CC-BY-NC-ND 4.0 International license.

739 incubation, the cultures were centrifuged at 8.000 × *g* for 15 min, washed with PBS, and
740 subjected to tenfold serial dilutions, starting from 10^7 cells/mL in PBS. Subsequently,
741 10 µL of each dilution was plated on Sabouraud agar (control) and Sabouraud agar
742 supplemented with fluconazole (1 - 6 µg/mL). Plates were incubated at 37 ºC for 96 h.

743 To further explore the effect of EVs on antifungal drug tolerance, a similar spot assay
744 was performed using *C. albicans* (fluconazole-susceptible) cultures (1×10^6 cells/mL).
745 These cultures were mixed with 100 µL of EVs (1×10^{10} EVs/mL) derived from a
746 fluconazole-resistant *C. auris* strain and incubated in 10 mL of Sabouraud broth at 37
747 ºC with shaking at 200 rpm for 24 h. Control cultures of *C. albicans* and *C. auris*
748 without EV treatment were also included. Following incubation, the cultures were
749 centrifuged, washed, and serially diluted tenfold. 10 µL of each dilution were plated on
750 Sabouraud agar and Sabouraud agar supplemented with fluconazole (1000 µg/mL).
751 Plates were incubated at 37 ºC for 96 h.

752

753 **Biofilm adhesion**

754 The effect of isolated EVs on biofilm adhesion was evaluated following the protocol
755 described by Zarnowski et al. (2021) (21), using a 96-well microplate assay. Each well
756 was inoculated with 1×10^6 cells of *C. albicans* or *C. auris* in RPMI medium. Different
757 concentrations of EVs (10-fold dilutions ranging from 10^9 to 10^5) were added to the
758 culture medium to assess their impact on biofilm formation. After 90 min of incubation
759 at 37 °C with 5% CO_2, the culture medium was carefully removed to eliminate non-
760 adherent cells. The biofilms were then washed with 100 µL of PBS. Biofilms adhesion
761 was quantified using the MTT (*Dimethyl-2-thiazol tetrazolium bromide*) assay. For this,
762 MTT was prepared in PBS at a final concentration of 0.5 mg/mL and protected from
763 light. A volume of 100 µL of this MTT solution was added to each well, and the plate
764 was incubated for 3 h at 37 ºC. Cellular dehydrogenase activity in living cells can be
765 followed by the reduction of MTT to formazan, a highly colored compound, due to the
766 action of NADH. The formazan crystals were then dissolved in 100 µL of DMSO
767 (*dimethyl sulfoxide*) was added, followed by an additional 10-min incubation at 37 ºC
768 with gentle shaking at 50 rpm. Absorbance was measured at 490 nm using a
769 SpectraMax 190 Microplate Reader spectrophotometer (Molecular Devices®).

bioRxiv preprint doi: https://doi.org/10.1101/2025.02.03.636213; this version posted February 4, 2025. The copyright holder for this preprint (which was not certified by peer review) is the author/funder, who has granted bioRxiv a license to display the preprint in perpetuity. It is made available under a CC-BY-NC-ND 4.0 International license.

The effect of EVs on biofilm adhesion of *C. neoformans* ΔCap67 was also evaluated based on protocols by Martinez et al. (2006) (57) and Benaducci (2016) (51), with modifications. Briefly, *C. neoformans* ΔCap67 was cultured overnight in Sabouraud broth at 37 °C with shaking at 200 rpm. Cells were then counted using a Neubauer chamber, centrifuged at 8.000 × *g* for 15 min, and resuspended in minimal medium (20 mg/mL thiamine, 30 mM glucose, 26 mM glycine, 20 mM $MgSO_4 \cdot 7H_2O$, 58.8 mM KH_2PO_4) to a final concentration of 1×10^7 cells/mL. In a 96-well microplate, 2×10^6 cells were added to each well and mixed with EVs at different concentrations (10-fold dilutions ranging from 10^9 to 10^5) in a final volume of 200 µL. After the adhesion stage, the supernatant was carefully aspirated and discarded, and biofilms were washed with PBS to remove non-adherent fungal cells. Biofilm adhesion was subsequently assessed using the MTT assay, following the procedure described above.

Biofilm dispersion

The impact of EVs on preformed *Candida* biofilms was assessed using a dispersion assay, following adapted protocols from Zarnowski et al. (2021) (21) and Zarnowski et al. (2022) (22). The assay was performed in 96-well microplates, with each well inoculated with 100 µL of a *C. albicans* or *C. auris* suspension (1×10^7 cells/mL) in RPMI medium. After a 90-min incubation at 37 °C with 5% CO_2, the culture medium was aspirated, and the biofilms were washed with 100 µL of PBS. Fresh RPMI medium was then added, and the biofilms were incubated for an additional 24 h under the same conditions. EVs isolated from *C. albicans* and *C. auris* were prepared at concentration ranging from 1×10^9 to 1×10^7 EVs/mL in RPMI medium - concentrations previously shown to affect the adhesion stage. These EV solutions were added to the preformed biofilms, followed by a 24-hour incubation. Afterward, supernatants containing detached cells were carefully transferred to a new microplate, where the quantity of dispersed cells was assessed using an MTT assay with the reagent at double concentration. Biofilm dispersion was analyzed by comparing EV-treated biofilms with untreated control biofilms.

The dispersion stage, characterized by the detachment of microcolonies or planktonic cells from mature *Cryptococcus* biofilms (86), was also evaluated in response to cryptococcal EVs. Following protocols adapted from studies on *Candida* biofilms (21,

bioRxiv preprint doi: https://doi.org/10.1101/2025.02.03.636213; this version posted February 4, 2025. The copyright holder for this preprint (which was not certified by peer review) is the author/funder, who has granted bioRxiv a license to display the preprint in perpetuity. It is made available under a CC-BY-NC-ND 4.0 International license.

22) and *Cryptococcus* biofilms (51, 57), a dispersion assay was performed in 96-well microplates. Each well was inoculated with 2×10^6 cells of *C. neoformans* ΔCap67 in minimal medium. After the initial adhesion stage, biofilms were washed with PBS to remove non-adherent cells and allowed to mature at 37 °C for 48 h in RPMI medium. The medium was then carefully replaced with suspensions containing 1×10^9 EVs from *C. neoformans* ΔCap67, *C. neoformans* H99 or *C. gattii* R265, diluted in RPMI. Following an additional 24-hour incubation, biofilm dispersion was quantified using the same MTT assay protocol applied to *Candida* biofilms.

Antifungal Susceptibility of Biofilms

Biofilm susceptibility to antifungal treatment was evaluated using a vesicle add-back assay, following the protocols described by Karkowska-Kuleta et al. (2023) (58) and Zarnowski et al. (2021) (21). Biofilms of *C. albicans* were established by inoculating 1×10^5 cells per well in a 96-well microplate. After a 90-min incubation at 37 ºC in a humidified atmosphere with 5% CO_2 to allow initial adhesion, the culture medium was aspirated, and biofilms were washed with PBS. Subsequently, 100 µL of RPMI medium containing EVs at concentrations of 1×10^9 EVs/mL were added to the wells, followed by a 2-hour incubation at 37 ºC. Fluconazole was then diluted in RPMI to a final concentration of 100 µg/mL and added to the wells, bringing the total volume to 200 µL per well. Control wells included biofilms without EV treatment. The microplates were incubated for 24 h at 37 ºC with 5% CO_2 in a humidified environment without agitation. Biofilm susceptibility to fluconazole was assessed using the MTT assay.

The influence of EVs on cell communication and antifungal susceptibility in *C. neoformans* ΔCap67 was evaluated using a microplate assay adapted from Martinez et al. (2006) (57) . *C. neoformans* ΔCap67 cells were cultured in Sabouraud liquid medium for 48 h at 37 °C with shaking at 200 rpm. The cultures were centrifuged at 8.000 × *g* for 15 min, and the resulting pellet was washed with PBS, centrifuged again, and resuspended in RPMI medium to a final concentration of 1×10^7 cells/mL. In a 96-well flat-bottom microplate, each well received 100 µL of the *C. neoformans* ΔCap67 suspension (1×10^7 cells/mL), 100 µL of EVs (1×10^9 EV/mL diluted in RPMI) derived from either *C. neoformans* or *C. gattii,* and 100 µL of antifungal agents (fluconazole at 10 µg/mL or amphotericin B at 5 µg/mL, both diluted in RPMI). The

bioRxiv preprint doi: https://doi.org/10.1101/2025.02.03.636213; this version posted February 4, 2025. The copyright holder for this preprint (which was not certified by peer review) is the author/funder, who has granted bioRxiv a license to display the preprint in perpetuity. It is made available under a CC-BY-NC-ND 4.0 International license.

834 microplates were incubated at 37 °C with shaking at 50 rpm for 72 h. Absorbance was
835 measured at 600 nm (OD_{600nm}) using a SpectraMax 190 Microplate Reader (Molecular
836 Devices®).

837

838 **Stimulation Assay of THP-1 macrophages with fungal EVs**

839 For the stimulation assay, 6-well plates were prepared with 1×10^6 THP-1 cells per
840 well, performed in triplicate. EVs were diluted in RPMI medium to a final concentration
841 of 1×10^9 EVs/mL, and 1 mL of this solution was added to each well, resulting in an
842 EV-to-macrophage ratio of 1000:1. Lipopolysaccharide (LPS) (Sigma®) at 100 ng/mL
843 was included as a positive control, while RPMI medium without EVs served as the
844 negative control. The plates were incubated for 20 h at 37 ºC with 5% CO_2. Following
845 incubation, supernatants were carefully collected and stored at –20 °C for subsequent
846 cytokine quantification. Cells were harvested using PBS, and total RNA was extracted
847 using the RNeasy Mini kit (Qiagen®) according to the manufacturer's protocol. RNA
848 concentration and purity were determined using a Nanodrop One spectrophotometer
849 (Thermo®), and the extracted RNA was stored at -80 °C for later qPCR analysis. To
850 evaluate the impact of EVs on THP-1 cells, cell size, viability, and concentration were
851 assessed using the Countess 3.0 Automated Cell Counter (Thermo®).

852

853 **Detection of Cytokine Production**

854 Culture supernatants were pooled according to the respective stimulus and stored at –20
855 °C until cytokine quantification via enzyme-linked immunosorbent assay (ELISA).
856 Human cytokine detection kits for TNFα, IL1β, IL4, IL6, IL8, and IL10 (BD
857 Biosciences®) were used following the manufacturer's instructions. Cytokine levels
858 were determined by measuring absorbance at 450 nm, with wavelength correction at
859 570 nm, using a SpectraMax 190 Microplate Reader (Molecular Devices®).

860

861 **Quantitative Real-time PCR (qPCR)**

862 For cDNA synthesis, 1 µg of total RNA obtained from the THP-1 stimulation assay was
863 reverse-transcribed using the High-capacity cDNA Reverse Transcription Kit (Applied

bioRxiv preprint doi: https://doi.org/10.1101/2025.02.03.636213; this version posted February 4, 2025. The copyright holder for this preprint (which was not certified by peer review) is the author/funder, who has granted bioRxiv a license to display the preprint in perpetuity. It is made available under a CC-BY-NC-ND 4.0 International license.

Biosystems®), following the manufacturer's protocol, including the recommended time and temperature conditions. Quantitative PCR (qPCR) was performed using the SyGreen Mix (PCR Biosystems®) in a final reaction volume of 10 µL per well, containing 50 ng of cDNA. Reactions were conducted on a StepOne Plus Real-time PCR system (Applied Biosystems®) under the following cycling conditions: initial denaturation at 95 °C for 2 min, followed by 40 cycles of 5 sec at 95 °C and 30 sec at 60 °C, as per PCR Biosystems ® recommendations. In the fungal communications experiments (fungal culture + EVs), the mRNA expression levels of *Erg11*, *Lac1*, *Ure1*, and *Cap59* were normalized to the housekeeping gene *18S rRNA*. Additionally, the immune response triggered by fungal EVs in THP-1 macrophage cultures was evaluated via qPCR by analyzing the expression of *TLR2, TLR4, TLR9, LGALS3* (Galectin-3), *CLEC7A,* (Dectin-1), *ARG1, iNOS, CGAS, STING, SYK, MYD88*, and *CARD9* (refer to Supplementary Table 1 for primers list). These genes were normalized against the housekeeping gene *ACT1* (β-Actin). Relative mRNA expression levels were calculated using the 2-ΔΔCT method, as described previously (87).

Statistical Analysis

Data analysis was performed using GraphPad Prism 9.0 (Dotmatics®). Statistical comparisons were conducted using either one-way or two-way ANOVA, depending on the experimental design. A p-value of $p < 0.05$ was considered statistically significant.

Acknowledgments

The authors thank Carlos Alberto Vieira, Maria Dolores Seabra Ferreira, and José Augusto Maulin for technical support. This study was financed, in part, by the São Paulo Research Foundation (FAPESP), Brazil. Process Number 2023/05800-7; 2021/06794-5.

Competing interest statement

The authors declare no conflict of interest.

bioRxiv preprint doi: https://doi.org/10.1101/2025.02.03.636213; this version posted February 4, 2025. The copyright holder for this preprint (which was not certified by peer review) is the author/funder, who has granted bioRxiv a license to display the preprint in perpetuity. It is made available under a CC-BY-NC-ND 4.0 International license.

894 **References**

895 1. Jafarlou M. 2024. Unveiling the menace: a thorough review of potential
896 pandemic fungal disease. Front Fungal Biol 5:1–9.

897 2. Rokas A. 2022. Evolution of the human pathogenic lifestyle in fungi. Nat
898 Microbiol 7:607–619.

899 3. Brown GD, Ballou ER, Bates S, Bignell EM, Borman AM, Brand AC, Brown
900 AJP, Coelho C, Cook PC, Farrer RA, Govender NP, Gow NAR, Hope W,
901 Hoving JC, Dangarembizi R, Harrison TS, Johnson EM, Mukaremera L,
902 Ramsdale M, Thornton CR, Usher J, Warris A, Wilson D. 2024. The
903 pathobiology of human fungal infections. Nat Rev Microbiol 11:687-704.

904 4. Seidel D, Wurster S, Jenks JD, Sati H, Gangneux JP, Egger M, Alastruey-
905 Izquierdo A, Ford NP, Chowdhary A, Sprute R, Cornely O, Thompson GR,
906 Hoenigl M, Kontoyiannis DP. 2024. Impact of climate change and natural
907 disasters on fungal infections. The Lancet Microbe 5:e594–e605.

908 5. Denning DW. 2024. Global incidence and mortality of severe fungal disease.
909 Lancet Infect Dis 24:e428–e438.

910 6. Inácio MM, Moreira ALE, Cruz-Leite VRM, Mattos K, Silva LOS, Venturini J,
911 Ruiz OH, Ribeiro-Dias F, Weber SS, Soares CM de A, Borges CL. 2023. Fungal
912 Vaccine Development: State of the Art and Perspectives Using
913 Immunoinformatics. J Fungi 9: 633-668.

914 7. Fisher MC, Denning DW. 2023. The WHO fungal priority pathogens list as a
915 game-changer. Nat Rev Microbiol 21:211–212.

916 8. Lionakis MS, Drummond RA, Hohl TM. 2023. Immune responses to human
917 fungal pathogens and therapeutic prospects. Nat Rev Immunol 23:433–452.

918 9. Chang CC, Harrison TS, Bicanic TA, Chayakulkeeree M, Sorrell TC, Warris A,
919 Hagen F, Spec A, Oladele R, Govender NP, Chen SC, Mody CH, Groll AH,
920 Chen YC, Lionakis MS, Alanio A, Castañeda E, Lizarazo J, Vidal JE, Takazono
921 T, Hoenigl M, Alffenaar JW, Gangneux JP, Soman R, Zhu LP, Bonifaz A, Jarvis
922 JN, Day JN, Klimko N, Salmanton-García J, Jouvion G, Meya DB, Lawrence D,
923 Rahn S, Bongomin F, McMullan BJ, Sprute R, Nyazika TK, Beardsley J,

bioRxiv preprint doi: https://doi.org/10.1101/2025.02.03.636213; this version posted February 4, 2025. The copyright holder for this preprint (which was not certified by peer review) is the author/funder, who has granted bioRxiv a license to display the preprint in perpetuity. It is made available under a CC-BY-NC-ND 4.0 International license.

924 Carlesse F, Heath CH, Ayanlowo OO, Mashedi OM, Queiroz-Telles Filho F,
925 Hosseinipour MC, Patel AK, Temfack E, Singh N, Cornely OA, Boulware DR,
926 Lortholary O, Pappas PG, Perfect JR. 2024. Global guideline for the diagnosis
927 and management of cryptococcosis: an initiative of the ECMM and ISHAM in
928 cooperation with the ASM. Lancet Infect Dis 24:e495–e512.

929 10. Rizzo J, Rodrigues ML, Janbon G. 2020. Extracellular Vesicles in Fungi: Past,
930 Present, and Future Perspectives. Front Cell Infect Microbiol 10:1–13.

931 11. de Oliveira HC, Castelli RF, Reis FCG, Rizzo J, Rodrigues ML. 2020.
932 Pathogenic delivery: The biological roles of cryptococcal extracellular vesicles.
933 Pathogens 9:1–14.

934 12. Welsh JA, Goberdhan DCI, O'Driscoll L, Buzas EI, Blenkiron C, Bussolati B,
935 Cai H, Di Vizio D, Driedonks TAP, Erdbrügger U, Falcon-Perez JM, Fu Q, Hill
936 AF, Lenassi M, Lim SK, Mahoney MG, Mohanty S, Möller A, Nieuwland R,
937 Ochiya T, Sahoo S, Torrecilhas AC, Zheng L, Zijlstra A, Abuelreich S, Bagabas
938 R, Bergese P, Bridges EM, Brucale M, Burger D, Carney RP, Cocucci E,
939 Crescitelli R, Hanser E, Harris AL, Haughey NJ, Hendrix A, Ivanov AR,
940 Jovanovic-Talisman T, Kruh-Garcia NA, Ku'ulei-Lyn Faustino V, Kyburz D,
941 Lässer C, Lennon KM, Lötvall J, Maddox AL, Martens-Uzunova ES, Mizenko
942 RR, Newman LA, Ridolfi A, Rohde E, Rojalin T, Rowland A, Saftics A, Sandau
943 US, Saugstad JA, Shekari F, Swift S, Ter-Ovanesyan D, Tosar JP, Useckaite Z,
944 Valle F, Varga Z, van der Pol E, van Herwijnen MJC, Wauben MHM, Wehman
945 AM, Williams S, Zendrini A, Zimmerman AJ, Théry C, Witwer KW. 2024.
946 Minimal information for studies of extracellular vesicles (MISEV2023): From
947 basic to advanced approaches. J Extracell Vesicles 13:e12404.

948 13. Bitencourt TA, Hatanaka O, Pessoni AM, Freitas MS, Trentin G, Santos P, Rossi
949 A, Martinez-Rossi NM, Alves LL, Casadevall A, Rodrigues ML, Almeida F.
950 2022. Fungal Extracellular Vesicles Are Involved in Intraspecies Intracellular
951 Communication. MBio 13:e03272-21.

952 14. Brauer VS, Pessoni AM, Bitencourt TA, Paula RG de, Rocha L de O, Gustavo H.
953 Goldman, Almeidaa F. 2020. Extracellular Vesicles from *Aspergillus flavus*
954 Induce M1 Polarization In Vitro. mSphere 5:e00190-20.

bioRxiv preprint doi: https://doi.org/10.1101/2025.02.03.636213; this version posted February 4, 2025. The copyright holder for this preprint (which was not certified by peer review) is the author/funder, who has granted bioRxiv a license to display the preprint in perpetuity. It is made available under a CC-BY-NC-ND 4.0 International license.

15. Freitas MS, Bitencourt TA, Rezende CP, Martins NS, Dourado T de MH, Tirapelli CR, Almeida F. 2023. *Aspergillus fumigatus* Extracellular Vesicles Display Increased *Ga lleria mellonella* Survival but Partial Pro-Inflammatory Response by Macrophages. J Fungi 9:541-556.

16. Oliveira BTM, Dourado TMH, Santos PWS, Bitencourt TA, Tirapelli CR, Colombo AL, Almeida F. 2023. Extracellular Vesicles from *Candida haemulonii* var. *vulnera* Modulate Macrophage Oxidative Burst. J Fungi 9:562-577.

17. Bitencourt TA, Rezende CP, Quaresemin NR, Moreno P, Hatanaka O, Rossi A, Martinez-Rossi NM, Almeida F. 2018. Extracellular vesicles from the dermatophyte *Trichophyton interdigitale* modulate macrophage and keratinocyte functions. Front Immunol 9:5–7.

18. Stotz HU, Brotherton D, Inal J. 2022. Communication is key: Extracellular vesicles as mediators of infection and defence during host-microbe interactions in animals and plants. FEMS Microbiol Rev 46:1–18.

19. Rodrigues ML, Casadevall A. 2018. A two-way road: novel roles for fungal extracellular vesicles. Mol Microbiol 110:11–15.

20. Honorato L, de Araujo JFD, Ellis CC, Piffer AC, Pereira Y, Frases S, de Sousa Araújo GR, Pontes B, Mendes MT, Pereira MD, Guimarães AJ, da Silva NM, Vargas G, Joffe L, Del Poeta M, Nosanchuk JD, Zamith-Miranda D, dos Reis FCG, de Oliveira HC, Rodrigues ML, de Toledo Martins S, Alves LR, Almeida IC, Nimrichter L. 2022. Extracellular Vesicles Regulate Biofilm Formation and Yeast-to-Hypha Differentiation in *Candida albicans*. MBio 13:e00301-22.

21. Zarnowski R, Noll A, Chevrette MG, Sanchez H, Jones R, Anhalt H, Fossen J, Jaromin A, Currie C, Nett JE, Mitchell A, Andes DR. 2021. Coordination of fungal biofilm development by extracellular vesicle cargo. Nat Commun 12:6235-6244.

22. Zarnowski R, Sanchez H, Jaromin A, Zarnowska UJ, Nett JE, Mitchell AP, Andes D. 2022. A common vesicle proteome drives fungal biofilm development. Proc Natl Acad Sci 119:1–12.

23. Bielska E, Sisquella MA, Aldeieg M, Birch C, O'Donoghue EJ, May RC. 2018. Pathogen-derived extracellular vesicles mediate virulence in the fatal human

bioRxiv preprint doi: https://doi.org/10.1101/2025.02.03.636213; this version posted February 4, 2025. The copyright holder for this preprint (which was not certified by peer review) is the author/funder, who has granted bioRxiv a license to display the preprint in perpetuity. It is made available under a CC-BY-NC-ND 4.0 International license.

pathogen *Cryptococcus gattii*. Nat Commun 9:1556-1565.

24. Rodrigues ML, Nakayasu ES, Oliveira DL, Nimrichter L, Nosanchuk JD, Almeida IC, Casadevall A. 2008. Extracellular vesicles produced by *Cryptococcus neoformans* contain protein components associated with virulence. Eukaryot Cell 7:58–67.

25. Rodrigues ML, Nimrichter L, Oliveira DL, Nosanchuk JD, Casadevall A. 2008. Vesicular trans-cell wall Transport in fungi: A mechanism for the delivery of virulence-associated macromolecules? Lipid Insights 2 1:27–40.

26. Kassi FK, Drakulovski P, Bellet V, Roger F, Chabrol A, Krasteva D, Doumbia A, Landman R, Kakou A, Reynes J, Delaporte E, Menan HEI, Bertout S. 2019. *Cryptococcus* genetic diversity and mixed infections in Ivorian HIV patients: A follow up study. PLoS Negl Trop Dis 13:1–20.

27. de Faria Ferreira M, Brito-Santos F, Henrique Nascimento Theodoro P, de Abreu Almeida M, Lazera M dos S, Trilles L. 2022. Mixed infection by *Cryptococcus neoformans* and *Cryptococcus gattii* and coinfection with paracoccidioidomycosis in PLHIV. Med Mycol Case Rep 35:48–50.

28. Ullah A, Huang Y, Zhao K, Hua Y, Ullah S, Rahman M ur, Wang J, Wang Q, Hu X, Zheng L. 2023. Characteristics and potential clinical applications of the extracellular vesicles of human pathogenic Fungi. BMC Microbiol 23:1–15.

29. Freitas MS, Bonato VLD, Pessoni AM, Rodrigues ML, Casadevall A, Almeida F. 2019. Fungal Extracellular Vesicles as Potential Targets for Immune Interventions. mSphere 4:1–9.

30. Vargas G, Rocha JDB, Oliveira DL, Albuquerque PC, Frases S, Santos SS, Nosanchuk JD, Gomes AMO, Medeiros LCAS, Miranda K, Sobreira TJP, Nakayasu ES, Arigi EA, Casadevall A, Guimaraes AJ, Rodrigues ML, Freire-de-Lima CG, Almeida IC, Nimrichter L. 2015. Compositional and immunobiological analyses of extracellular vesicles released by *Candida albicans*. Cell Microbiol 17:389–407.

31. de Rezende CP, Santos PWS, Piraine RA, Silvestrini VC, Barbosa JCJ, Valera FCP, Tamashiro E, Podolski-Gondim GG, Quintana SM, Calado R, Martinez R, P. Fill T, Rodrigues ML, Almeida F. 2024. Extracellular vesicles produced

bioRxiv preprint doi: https://doi.org/10.1101/2025.02.03.636213; this version posted February 4, 2025. The copyright holder for this preprint (which was not certified by peer review) is the author/funder, who has granted bioRxiv a license to display the preprint in perpetuity. It is made available under a CC-BY-NC-ND 4.0 International license.

1017 during fungal infection in humans are immunologically active. bioRxiv (*preprint*)
1018 https://doi.org/10.1101/2024.03.20.585987.

1019 32. Lai Y, Jiang B, Hou F, Huang X, Ling B, Lu H, Zhong T, Huang J. 2023. The
1020 emerging role of extracellular vesicles in fungi: a double-edged sword. Front
1021 Microbiol 14:1–15.

1022 33. Oliveira DL, Freire-de-Lima CG, Nosanchuk JD, Casadevall A, Rodrigues ML,
1023 Nimrichter L. 2010. Extracellular vesicles from *Cryptococcus neoformans*
1024 modulate macrophage functions. Infect Immun 78:1601–1609.

1025 34. Marina CL, Bürgel PH, Agostinho DP, Zamith-Miranda D, Las-Casas L de O,
1026 Tavares AH, Nosanchuk JD, Bocca AL. 2020. Nutritional conditions modulate *C.*
1027 *neoformans* extracellular vesicles' capacity to elicit host immune response.
1028 Microorganisms 8:1–17.

1029 35. de Jesus M, Chow SK, Cordero RJB, Frases S, Casadevall A. 2010.
1030 Galactoxylomannans from *Cryptococcus neoformans* varieties neoformans and
1031 grubii are structurally and antigenically variable. Eukaryot Cell 9:1018–1028.

1032 36. Chang YC, Kwon-Chung KJ. 1994. Complementation of a Capsule-Deficient
1033 Mutation of *Cryptococcus neoformans* Restores its Virulence . Mol Cell Biol
1034 14:4912–4919.

1035 37. Zapparata A, Baroncelli R, Brandström Durling M, Kubicek CP, Karlsson M,
1036 Vannacci G, Sarrocco S. 2021. Fungal cross-talk: an integrated approach to study
1037 distance communication. Fungal Genet Biol 148:103518-103529.

1038 38. Cottier F, Mühlschlegel FA. 2012. Communication in fungi. Int J Microbiol
1039 2012:1-9.

1040 39. Reis FCG, Borges BS, Jozefowicz LJ, Sena BAG, Garcia AWA, Medeiros LC,
1041 Martins ST, Honorato L, Schrank A, Vainstein MH, Kmetzsch L, Nimrichter L,
1042 Alves LR, Staats CC, Rodrigues ML. 2019. A Novel Protocol for the Isolation of
1043 Fungal Extracellular Vesicles Reveals the Participation of a Putative Scramblase
1044 in Polysaccharide Export and Capsule Construction in *Cryptococcus gattii*.
1045 mSphere 4:e00080-19.

1046 40. Chan W, Chow FWN, Tsang CC, Liu X, Yao W, Chan TTY, Siu GKH, Ho

bioRxiv preprint doi: https://doi.org/10.1101/2025.02.03.636213; this version posted February 4, 2025. The copyright holder for this preprint (which was not certified by peer review) is the author/funder, who has granted bioRxiv a license to display the preprint in perpetuity. It is made available under a CC-BY-NC-ND 4.0 International license.

AYM, Luk KS, Lau SKP, Woo PCY. 2022. Induction of amphotericin B resistance in susceptible *Candida auris* by extracellular vesicles. Emerg Microbes Infect 11:1900–1909.

41. Rodrigues ML, May RC, Janbon G. 2024. The multiple frontiers in the study of extracellular vesicles produced by fungi. Microbes Infect 26:105233-105239.

42. Reis FCG, Gimenez B, Jozefowicz LJ, Castelli RF, Martins ST, Alves LR, de Oliveira HC, Rodrigues ML. 2021. Analysis of Cryptococcal Extracellular Vesicles: Experimental Approaches for Studying Their Diversity Among Multiple Isolates, Kinetics of Production, Methods of Separation, and Detection in Cultures of Titan Cells. Microbiol Spectr 9:e00125-21.

43. Rodrigues ML, Nimrichter L. 2022. From fundamental biology to the search for innovation: The story of fungal extracellular vesicles. Eur J Cell Biol 101:151205-151211.

44. Kulig K, Bednaruk K, Rudolphi-Szydło E, Barbasz A, Wronowska E, Barczyk-Woznicka O, Karnas E, Pyza E, Zuba-Surma E, Rapala-Kozik M, Karkowska-Kuleta J. 2023. Stress Conditions Affect the Immunomodulatory Potential of *Candida albicans* Extracellular Vesicles and Their Impact on Cytokine Release by THP-1 Human Macrophages. Int J Mol Sci 24:17179-17196.

45. Fröhlich E. 2012. The role of surface charge in cellular uptake and cytotoxicity of medical nanoparticles. Int J Nanomedicine 7:5577-5591.

46. Dietz L, Oberländer J, Mateos-Maroto A, Schunke J, Fichter M, Krämer-Albers EM, Landfester K, Mailänder V. 2023. Uptake of extracellular vesicles into immune cells is enhanced by the protein corona. J Extracell Vesicles 12:e12399.

47. Liam-Or R, Faruqu FN, Walters A, Han S, Xu L, Wang JTW, Oberlaender J, Sanchez-Fueyo A, Lombardi G, Dazzi F, Mailaender V, Al-Jamal KT. 2024. Cellular uptake and in vivo distribution of mesenchymal-stem-cell-derived extracellular vesicles are protein corona dependent. Nat Nanotechnol 19:846–855.

48. Walker L, Sood P, Lenardon MD, Milne G, Olson J, Jensen G, Wolf J, Casadevall A, Adler-Moore J, Gow NAR. 2018. The viscoelastic properties of the fungal cell wall allow traffic of ambisome as intact liposome vesicles. MBio

bioRxiv preprint doi: https://doi.org/10.1101/2025.02.03.636213; this version posted February 4, 2025. The copyright holder for this preprint (which was not certified by peer review) is the author/funder, who has granted bioRxiv a license to display the preprint in perpetuity. It is made available under a CC-BY-NC-ND 4.0 International license.

9:e02383-17.

49. Rodrigues ML, Nimrichter L, Oliveira DL, Frases S, Miranda K, Zaragoza O, Alvarez M, Nakouzi A, Feldmesser M, Casadevall A. 2007. Vesicular polysaccharide export in *Cryptococcus neoformans* is a eukaryotic solution to the problem of fungal trans-cell wall transport. Eukaryot Cell 6:48–59.

50. Salas SD, Bennett JE, Kwon-Chung KJ, Perfect JR, Williamson PR. 1996. Effect of the laccase gene, CNLAC1, on virulence of *Cryptococcus neoformans*. J Exp Med 184:377–386.

51. Benaducci T, Sardi J de CO, Lourencetti NMS, Scorzoni L, Gullo FP, Rossi SA, Derissi JB, de Azevedo Prata MC, Fusco-Almeida AM, Mendes-Giannini MJS. 2016. Virulence of *Cryptococcus* sp. biofilms in vitro and in vivo using *Galleria mellonella* as an alternative model. Front Microbiol 7:1–10.

52. Rybak JM, Cuomo CA, David Rogers P. 2022. The molecular and genetic basis of antifungal resistance in the emerging fungal pathogen *Candida auris*. Curr Opin Microbiol 70:102208-102216.

53. García-Rivera J, Chang YC, Kwon-Chung KJ, Casadevall A. 2004. *Cryptococcus neoformans* CAP59 (or Cap59p) is involved in the extracellular trafficking of capsular glucuronoxylomannan. Eukaryot Cell 3:385–392.

54. Wang D, Zeng N, Li C, Li Z, Zhang N, Li B. 2024. Fungal biofilm formation and its regulatory mechanism. Heliyon 10:e32766.

55. Tronchin G, Pihet M, Lopes-Bezerra L, Bouchara JP. 2008. Adherence mechanisms in human pathogenic fungi. Med Mycol 46:749–772.

56. Zarnowski R, Massey J, Mitchell AP, Andes D. 2022. Extracellular Vesicles Contribute to Mixed-Fungal Species Competition during Biofilm Initiation. MBio 13:e02988-22.

57. Martinez LR, Casadevall A. 2006. Susceptibility of *Cryptococcus neoformans* biofilms to antifungal agents in vitro. Antimicrob Agents Chemother 50:1021–1033.

58. Karkowska-Kuleta J, Kulig K, Bras G, Stelmaszczyk K, Surowiec M, Kozik A, Karnas E, Barczyk-Woznicka O, Zuba-Surma E, Pyza E, Rapala-Kozik M. 2023.

bioRxiv preprint doi: https://doi.org/10.1101/2025.02.03.636213; this version posted February 4, 2025. The copyright holder for this preprint (which was not certified by peer review) is the author/funder, who has granted bioRxiv a license to display the preprint in perpetuity. It is made available under a CC-BY-NC-ND 4.0 International license.

Candida albicans Biofilm-Derived Extracellular Vesicles Are Involved in the Tolerance to Caspofungin, Biofilm Detachment, and Fungal Proteolytic Activity. J Fungi 9:1078-1095.

59. Brandt P, Singha R, Ene I V. 2024. Hidden allies: how extracellular vesicles drive biofilm formation, stress adaptation, and host–immune interactions in human fungal pathogens. MBio 30:1163–1169.

60. Zarnowski R, Sanchez H, Covelli AS, Dominguez E, Jaromin A, Bernhardt J, Mitchell KF, Heiss C, Azadi P, Mitchell A, Andes DR. 2018. *Candida albicans* biofilm–induced vesicles confer drug resistance through matrix biogenesis. PLoS Biol 16:1–18.

61. Rodrigues ML, Janbon G. 2021. Fungal Extracellular Vesicles: Biological roles. In: Current Topics in Microbiology and Immunology. 1ed, vol 432: 333-340. Springer International Publishing, Cham.

62. Kwaku GN, Ward RA, Vyas JM, Brown Harding H. 2024. Host innate immune systems gather intel on invading microbes via pathogen-derived extracellular vesicles. Extracell Vesicle 3:100043-100053.

63. Oliveira-Brito PKM, Rezende CP, Almeida F, Roque-Barreira MC, da Silva TA. 2020. iNOS/Arginase-1 expression in the pulmonary tissue over time during *Cryptococcus gattii* infection. Innate Immun 26:117–129.

64. Strizova Z, Benesova I, Bartolini R, Novysedlak R, Cecrdlova E, Foley LK, Striz I. 2023. M1/M2 macrophages and their overlaps - myth or reality? Clin Sci 137:1067–1093.

65. Wang L xun, Zhang S xi, Wu H juan, Rong X lu, Guo J. 2019. M2b macrophage polarization and its roles in diseases. J Leukoc Biol 106:345–358.

66. Arranz A, Doxaki C, Vergadi E, De La Torre YM, Vaporidi K, Lagoudaki ED, Ieronymaki E, Androulidaki A, Venihaki M, Margioris AN, Stathopoulos EN, Tsichlis PN, Tsatsanis C. 2012. Akt1 and Akt2 protein kinases differentially contribute to macrophage polarization. Proc Natl Acad Sci U S A 109:9517–9522.

67. Zamith-Miranda D, Heyman HM, Couvillion SP, Cordero RJB, Rodrigues ML,

bioRxiv preprint doi: https://doi.org/10.1101/2025.02.03.636213; this version posted February 4, 2025. The copyright holder for this preprint (which was not certified by peer review) is the author/funder, who has granted bioRxiv a license to display the preprint in perpetuity. It is made available under a CC-BY-NC-ND 4.0 International license.

1138 Nimrichter L, Casadevall A, Amatuzzi RF, Alves LR, Nakayasu ES, Nosanchuk
1139 JD. 2021. Comparative Molecular and Immunoregulatory Analysis of
1140 Extracellular Vesicles from *Candida albicans* and *Candida auris.* mSystems
1141 6:e00822-21.

1142 68. Da Silva TA, Roque-Barreira MC, Casadevall A, Almeida F. 2016. Extracellular
1143 vesicles from *Paracoccidioides brasiliensis* induced M1 polarization in vitro. Sci
1144 Rep 6:1–10.

1145 69. Honorato L, Bonilla JJA, Valdez AF, Frases S, Araújo GR de S, Sabino ALR do
1146 N, da Silva NM, Ribeiro L, Ferreira M da S, Kornetz J, Rodrigues ML,
1147 Cunningham I, Gow NAR, Gacser A, Guimarães AJ, Dutra FF, Nimrichter L.
1148 2024. Toll-like receptor 4 (TLR4) is the major pattern recognition receptor
1149 triggering the protective effect of a *Candida albicans* extracellular vesicle-based
1150 vaccine prototype in murine systemic candidiasis. mSphere 9:1–19.

1151 70. Montanari Borges B, Gama de Santana M, Willian Preite N, de Lima Kaminski
1152 V, Trentin G, Almeida F, Vieira Loures F. 2024. Extracellular vesicles from
1153 virulent *P. brasiliensis* induce TLR4 and dectin-1 expression in innate cells and
1154 promote enhanced Th1/Th17 response. Virulence 15: 2329573.

1155 71. Pruksaphon K, Amsri A, Thammasit P, Nosanchuk JD, Youngchim S. 2023.
1156 Extracellular vesicles derived from *Talaromyces marneffei* contain immunogenic
1157 compounds and modulate THP-1 macrophage responses. Front Immunol 14:1–
1158 13.

1159 72. Vargas G, Honorato L, Guimarães AJ, Rodrigues ML, Reis FCG, Vale AM, Ray
1160 A, Nosanchuk JD, Nimrichter L. 2020. Protective effect of fungal extracellular
1161 vesicles against murine candidiasis. Cell Microbiol 22:1–15.

1162 73. da Silva-Junior EB, Firmino-Cruz L, Guimarães-de-Oliveira JC, De-Medeiros
1163 JVR, de Oliveira Nascimento D, Freire-de-Lima M, de Brito-Gitirana L, Morrot
1164 A, Previato JO, Mendonça-Previato L, Decote-Ricardo D, de Matos Guedes HL,
1165 Freire-de-Lima CG. 2021. The role of Toll-like receptor 9 in a murine model of
1166 *Cryptococcus gattii* infection. Sci Rep 11:1–11.

1167 74. Almeida F, Wolf JM, Da Silva TA, Deleon-Rodriguez CM, Rezende CP, Pessoni
1168 AM, Fernandes FF, Silva-Rocha R, Martinez R, Rodrigues ML, Roque-Barreira

bioRxiv preprint doi: https://doi.org/10.1101/2025.02.03.636213; this version posted February 4, 2025. The copyright holder for this preprint (which was not certified by peer review) is the author/funder, who has granted bioRxiv a license to display the preprint in perpetuity. It is made available under a CC-BY-NC-ND 4.0 International license.

MC, Casadevall A. 2017. Galectin-3 impacts *Cryptococcus neoformans* infection through direct antifungal effects. Nat Commun 8:1–13.

75. Hatanaka O, Rezende CP, Moreno P, Freitas Fernandes F, Oliveira Brito PKM, Martinez R, Coelho C, Roque-Barreira MC, Casadevall A, Almeida F. 2019. Galectin-3 Inhibits *Paracoccidioides brasiliensis* Growth and Impacts Paracoccidioidomycosis through Multiple Mechanisms. mSphere 4:1–10.

76. Zajta E, Csonka K, Tóth A, Tiszlavicz L, Németh T, Orosz A, Novák Á, Csikós M, Vágvölgyi C, Mócsai A, Gácser A. 2021. Signaling through Syk or CARD9 Mediates Species-Specific Anti- *Candida* Protection in Bone Marrow Chimeric Mice. MBio 12:e01608-21.

77. Bi L, Gojestani S, Wu W, Hsu YMS, Zhu J, Ariizumi K, Lin X. 2010. CARD9 mediates dectin-2-induced IκBα kinase ubiquitination leading to activation of NF-κB in response to stimulation by the hyphal form of *Candida albicans*. J Biol Chem 285:25969–25977.

78. Gu Y, Jia XM. 2023. STING negatively regulates antifungal immunity. Trends Microbiol 31:1090–1092.

79. Chen T, Feng Y, Sun W, Zhao G, Wu H, Cheng X, Zhao F, Zhang L, Zheng Y, Zhan P, Zhao W, Liu B, Gao C. 2023. The nucleotide receptor STING translocates to the phagosomes to negatively regulate anti-fungal immunity. Immunity 56:1727-1742.

80. Brown Harding H, Kwaku GN, Reardon CM, Khan NS, Zamith-Miranda D, Zarnowski R, Tam JM, Bohaen CK, Richey L, Mosallanejad K, Crossen AJ, Reedy JL, Ward RA, Vargas-Blanco DA, Basham KJ, Bhattacharyya RP, Nett JE, Mansour MK, van de Veerdonk FL, Kumar V, Kagan JC, Andes DR, Nosanchuk JD, Vyas JM. 2024. *Candida albicans* extracellular vesicles trigger type I IFN signalling via cGAS and STING. Nat Microbiol 9:95–107.

81. Freitas MS, Pessoni AM, Coelho C, Bonato VLD, Rodrigues ML, Casadevall A, Almeida F. 2021. Interactions of Extracellular Vesicles from Pathogenic Fungi with Innate Leukocytes, 1ed, vol432: p. 89–120. *In* Current Topics in Microbiology and Immunology. Springer.

82. Peng M, Li X, Zhang X, Peng L. 2023. Inhibition of cGAS aggravated the host

bioRxiv preprint doi: https://doi.org/10.1101/2025.02.03.636213; this version posted February 4, 2025. The copyright holder for this preprint (which was not certified by peer review) is the author/funder, who has granted bioRxiv a license to display the preprint in perpetuity. It is made available under a CC-BY-NC-ND 4.0 International license.

inflammatory response to *Aspergillus fumigatus*. Exp Lung Res 49:86–100.

83. Kulig K, Karnas E, Woznicka O, Kuleta P, Zuba-Surma E, Pyza E, Osyczka A, Kozik A, Rapala-Kozik M, Karkowska-Kuleta J. 2022. Insight Into the Properties and Immunoregulatory Effect of Extracellular Vesicles Produced by C*andida glabrata*, *Candida parapsilosis*, and *Candida tropicalis* Biofilms. Front Cell Infect Microbiol 12:1–13.

84. Liu J, Hu X. 2023. Fungal extracellular vesicle-mediated regulation: from virulence factor to clinical application. Front Microbiol 14:1205477.

85. Rizzo J, Trottier A, Moyrand F, Coppée J, Maufrais C, Zimbres ACG, Dang TTV, Alanio A, Desnos-Ollivier M, Mouyna I, Péhau-Arnaude G, Commere P, Novault S, Ene I V, Nimrichter L, Rodrigues ML, Janbon G. 2023. Coregulation of extracellular vesicle production and fluconazole susceptibility in *Cryptococcus neoformans*. MBio 0:1–22.

86. Lopes W, Vainstein MH, Araujo GRDS, Frases S, Staats CC, de Almeida RMC, Schrank A, Kmetzsch L, Vainstein MH. 2017. Geometrical distribution of *Cryptococcus neoformans* mediates flower-like biofilm development. Front Microbiol 8:1–13.

87. Livak KJ, Schmittgen TD. 2001. Analysis of relative gene expression data using real-time quantitative PCR and the 2-ΔΔCT method. Methods 25:402–408.

bioRxiv preprint doi: https://doi.org/10.1101/2025.02.03.636213; this version posted February 4, 2025. The copyright holder for this preprint (which was not certified by peer review) is the author/funder, who has granted bioRxiv a license to display the preprint in perpetuity. It is made available under a CC-BY-NC-ND 4.0 International license.

FIGURE LEGENDS

Figure 1: Characterization of fungal extracellular vesicles (EVs). EVs isolated from *C. albicans* ATCC 64548 (A), *C. auris* 470/2015 (B), *C. neoformans* H99 (C), and *C. gattii* R265 (D) were analyzed by Nanoparticle Tracking Analysis (NTA). The data obtained from NTA is summarized in panel (E). Zeta potential measurements of EVs were performed using Dynamic Light Scattering and are shown in panel (F). Statistical analysis was conducted using One-way ANOVA in GraphPad Prism 9.0. Error bars represent mean ± standard deviation.

Figure 2: Interspecies cell surface association and internalization of fungal EVs. (A) Fluorescence microscopy images suggest that fungal cells are capable of recognizing, interacting with, and possibly internalizing EVs produced by different species and genera. Yellow arrows indicate cells that are internalizing EVs, at 400 × magnification. SEM images show the association of fungal EVs (indicated in yellow) with the cell wall after co-incubation with *C. albicans* (A) and *C. neoformans* ΔCap67 (B), demonstrating interspecies interactions between EVs and fungal cells. Images "b" and "d" in both experiments (for *Candida* spp. and *Cryptococcus* spp.) were manually colored using GIMP2® software to correspond to images "a" and "c". Magnification of 20,000x.

Figure 3: Biological impact of EVs derived from *C. neoformans* and *C. gattii* on planktonic cells and biofilms. Planktonic cells of *C. neoformans* ΔCap67 were incubated with EVs isolated from *C. neoformans* H99 and *C. gattii* R265. mRNA relative expression levels of *Cap59 (*A), *Lac1* (B), and *Ure1* (C) were measured by qPCR and compared to the control (no EV treatment). The dotted lines represent the basal expression in *C. neoformans* ΔCap67 cultures. (D) A dot blot was used to detect the presence of the capsular content GXM in fungal EVs. BSA 5% served as a negative control (-), while *Cn*: *C. neoformans* H99, and *Cg*: *C. gattii* R265 cultures were used as positive controls. (E) Dot blot analysis of ΔCap67 cultures incubated with EVs from *C. neoformans* H99 and *C. gattii* R265, showing a positive reaction with the anti-GXM monoclonal antibody. (F-H) EVs from *C. neoformans* ΔCap67, *C. neoformans* H99, and *C. gattii* R265, at concentrations ranging from 10^4 to 10^8 EVs/well, were added to biofilms of *C. neoformans* ΔCap67. Biofilm adhesion was evaluated at each EV concentration, and the concentration with the most pronounced biological effect was selected for further analysis of biofilm dispersion (I) and susceptibility to fluconazole and amphotericin B (J). The dotted lines represent the biofilm formed by non-treated *C. neoformans* ΔCap67 (no EVs added). Statistical analysis was performed using One-way ANOVA in GraphPad Prism 9.0, with significant differences indicated by the "*" symbol: *$p < 0.05$, **$p < 0.01$, ***$p < 0.001$, and ****$p < 0.0001$. Error bars represent means ± standard deviation. (K) Spot tests were conducted with dilutions of *C. neoformans* ΔCap67 cultures, with or without EVs (control), to assess the effect on antifungal tolerance in planktonic cells.

bioRxiv preprint doi: https://doi.org/10.1101/2025.02.03.636213; this version posted February 4, 2025. The copyright holder for this preprint (which was not certified by peer review) is the author/funder, who has granted bioRxiv a license to display the preprint in perpetuity. It is made available under a CC-BY-NC-ND 4.0 International license.

Figure 4: Biological impact of EVs from *C. albicans* and *C. auris* on planktonic cells and biofilms. (A) Planktonic *C. albicans* cells were incubated with EVs isolated from *C. albicans*, *C. auris*, or *C. auris* treated with fluconazole. *Erg11* mRNA relative expression was measured by qPCR and compared to the control (no EV treatment). The dotted line represents the basal expression in *C. albicans* cultures. (B) Spot tests were conducted with dilutions of *C. albicans* cultures that were treated with or without EVs (control strain: *C. albicans* and *C. auris*) on Sabouraud agar plates with or without fluconazole. (C) Fluconazole susceptibility in *C. albicans* (a fluconazole-susceptible strain) biofilms was tested following the addition of *C. albicans* EVs or *C. auris* EVs (10^9 EVs/mL). (D, E, and F) Different concentrations of EVs from *C. albicans* and *C. auris* were added on adhesion and dispersion phase of *C. albicans* biofilms. (G, H, and I) Different concentrations of EVs from *C. albicans* and *C. auris* were added on adhesion and dispersion phase of *C. auris* biofilms. Biofilm dispersion was assessed after adding EVs to pre-formed biofilms of both *Candida* species. For all biofilm assays, the dotted lines represent results for biofilms with no EV addition. Statistical analysis was performed using One-way ANOVA in GraphPad Prism 9.0, with significant differences indicated by the "*" symbol: *$p < 0.05$, **$p < 0.01$, ***$p < 0.001$, and ****$p < 0.0001$. Error bars represent means ± standard deviation.

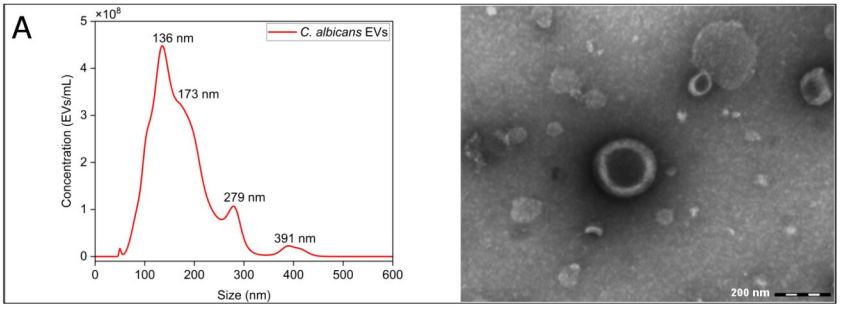
Figure 5: Interaction between fungal EVs and THP-1 macrophages, and its impact on cellular properties. (A) The internalization of EVs by THP-1 cells was observed through fluorescence microscopy, demonstrating successful recognition and interaction with human macrophages. Micrographs from bright field and under fluorescence (560 nm) were merged using GIMP® 2 software. The biological effects on THP-1 cells following EV interaction were assessed by measuring the number of live cells (B), cell size (C), and cell concentration (D). Dotted lines indicated the data observed for untreated cells (control).

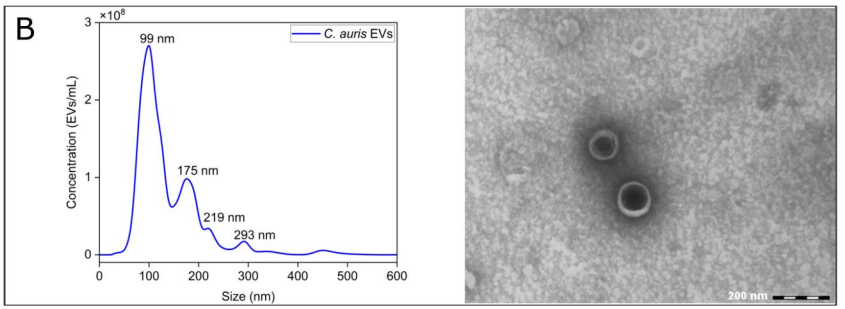
Figure 6: Relative mRNA expression of polarization markers, receptors, and signaling pathway proteins in THP-1 cells stimulated with fungal EVs. This figure presents the relative expression levels of macrophage polarization markers (*iNOS*, *ARG1*), receptors (*TLR2*, *TLR4*, *TLR9*, *CLEC7A*, *LGALS3*), and proteins involved in key immune signaling cascades (*STING*, *CGAS*, *CARD9*, *SYK*, *MYD88*). qPCR results were normalized to the housekeeping β-actin gene (*ACT1*) and calculated using the 2-ΔΔCT method. The heatmap presented in (A) summarizes the results observed for relative mRNA transcription. Fold change for relative mRNA transcription is presented in the graphs (B-M) as $\log_2$, to facilitate up- and downregulation comparisons.

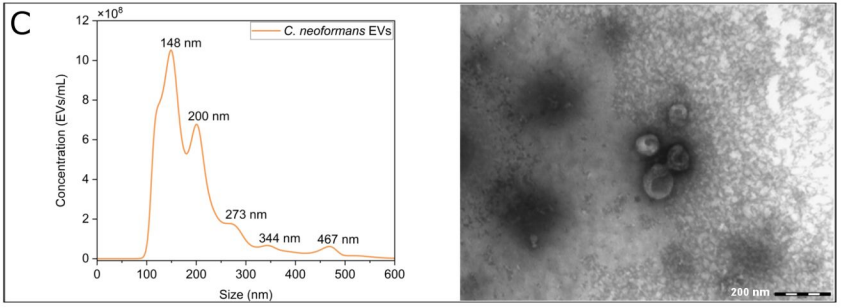
Figure 7: Cytokine production by THP-1 macrophages following stimulation with fungal EVs. THP-1 cells were cultured either with medium only (control) or with EVs derived from *C. albicans*, *C. auris*, *C. neoformans*, and *C. gattii*. The production of IL-1β (A), IL-4 (B), IL-6 (C), L-8 (D), IL-10 (E), and TNFα (F) was quantified by ELISA. Statistical analysis was performed using GraphPad Prism 9.0

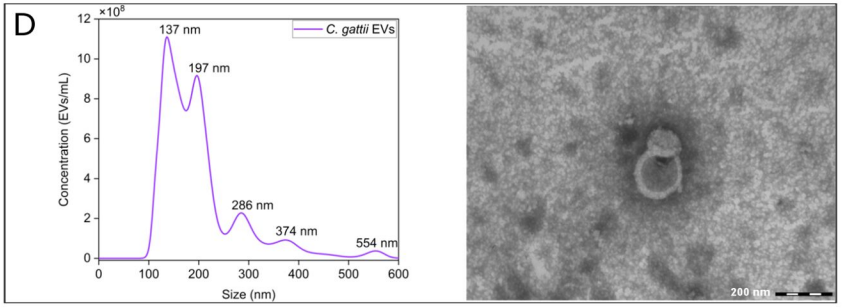
bioRxiv preprint doi: https://doi.org/10.1101/2025.02.03.636213; this version posted February 4, 2025. The copyright holder for this preprint (which was not certified by peer review) is the author/funder, who has granted bioRxiv a license to display the preprint in perpetuity. It is made available under a CC-BY-NC-ND 4.0 International license.

with a One-way ANOVA test. Significant differences are indicated by *p*-values above the bars, compared to the control (medium only). Error bars represent the means ± standard deviation.



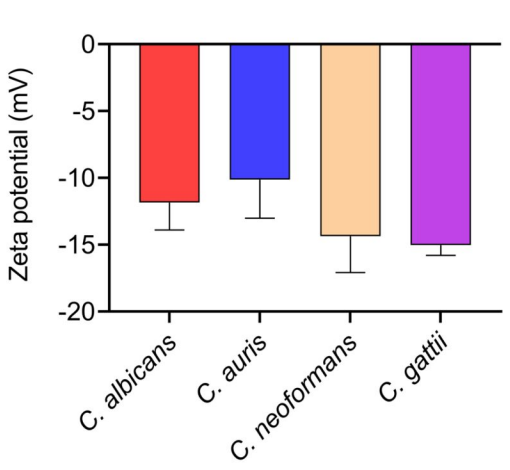


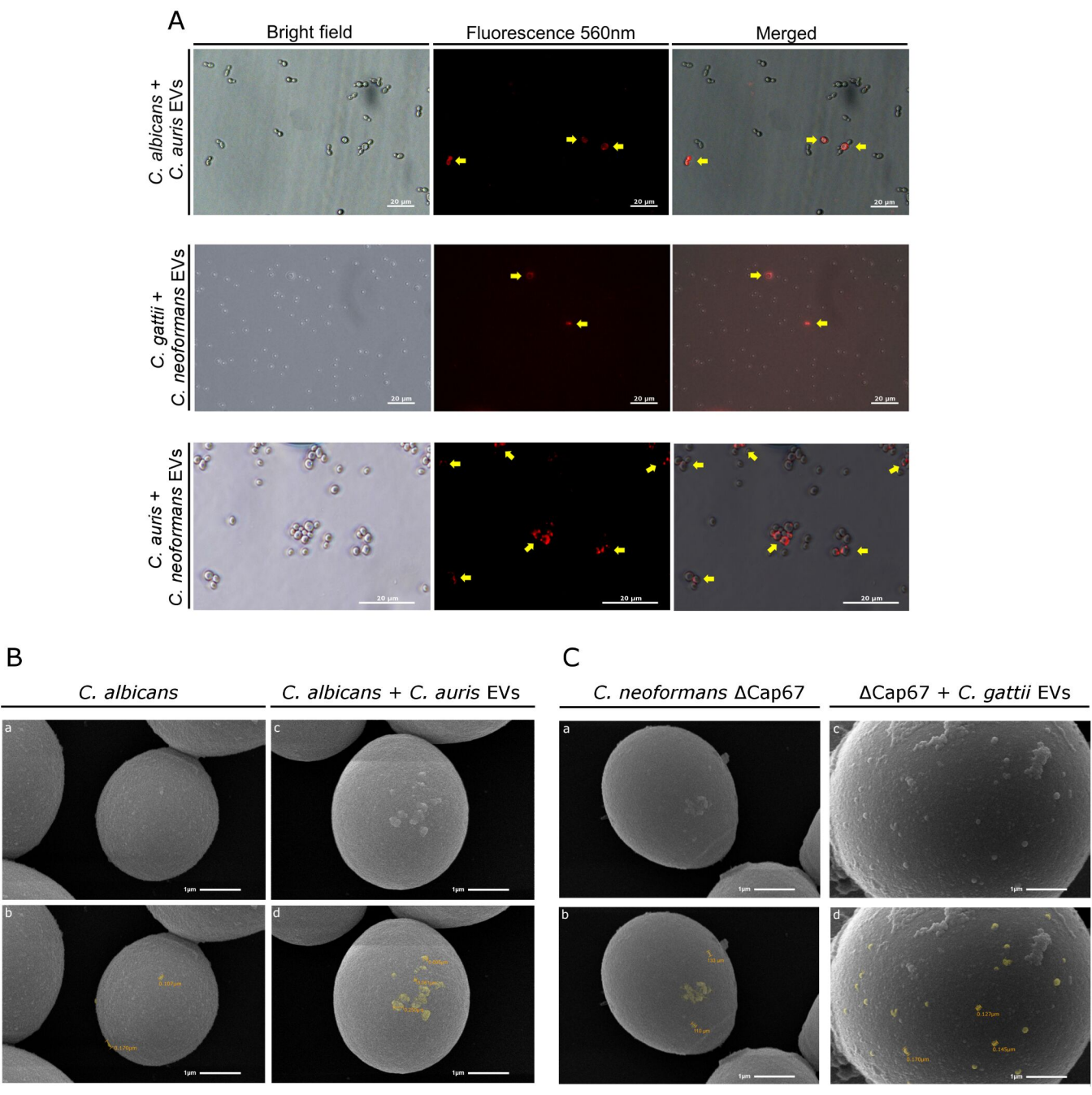


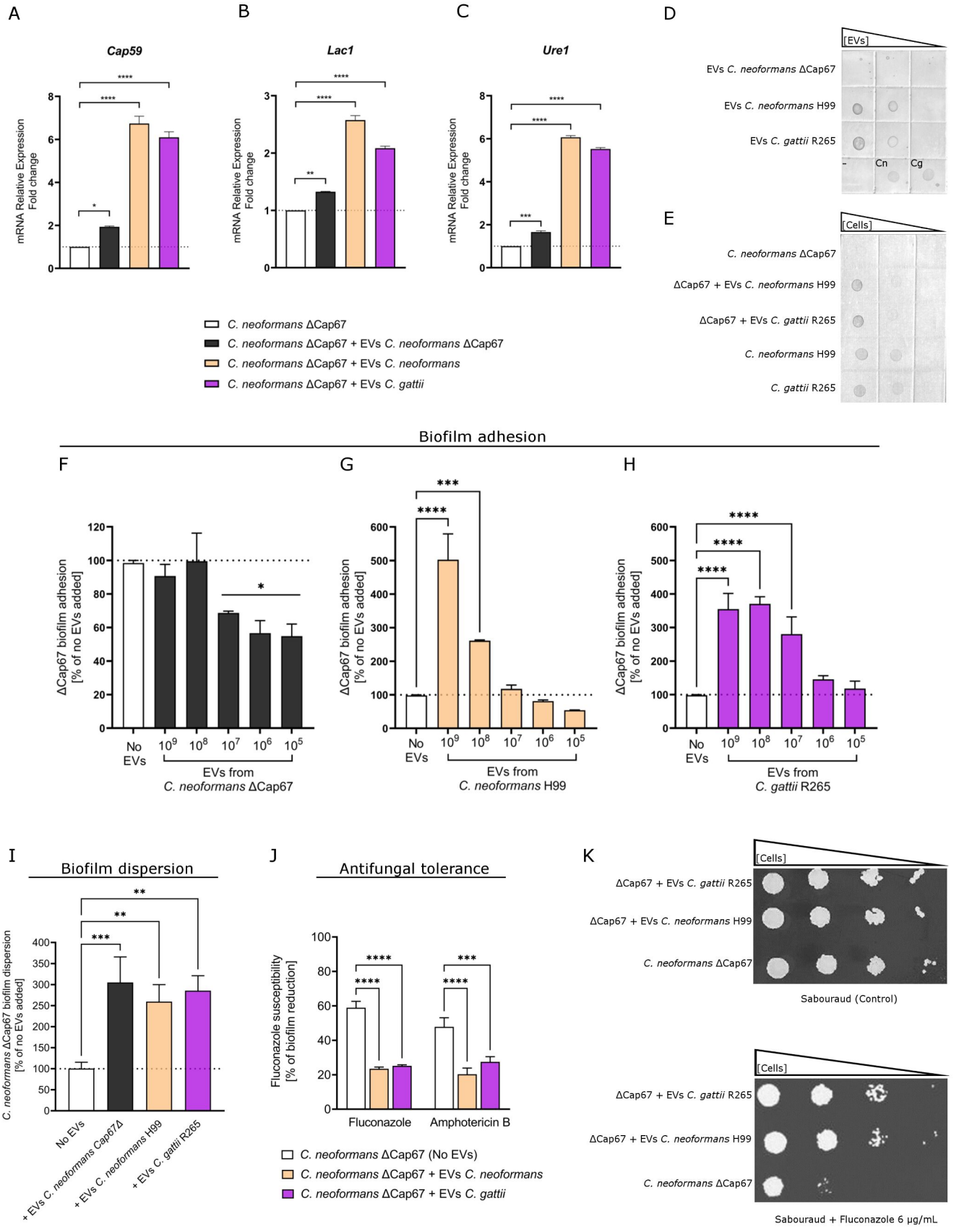


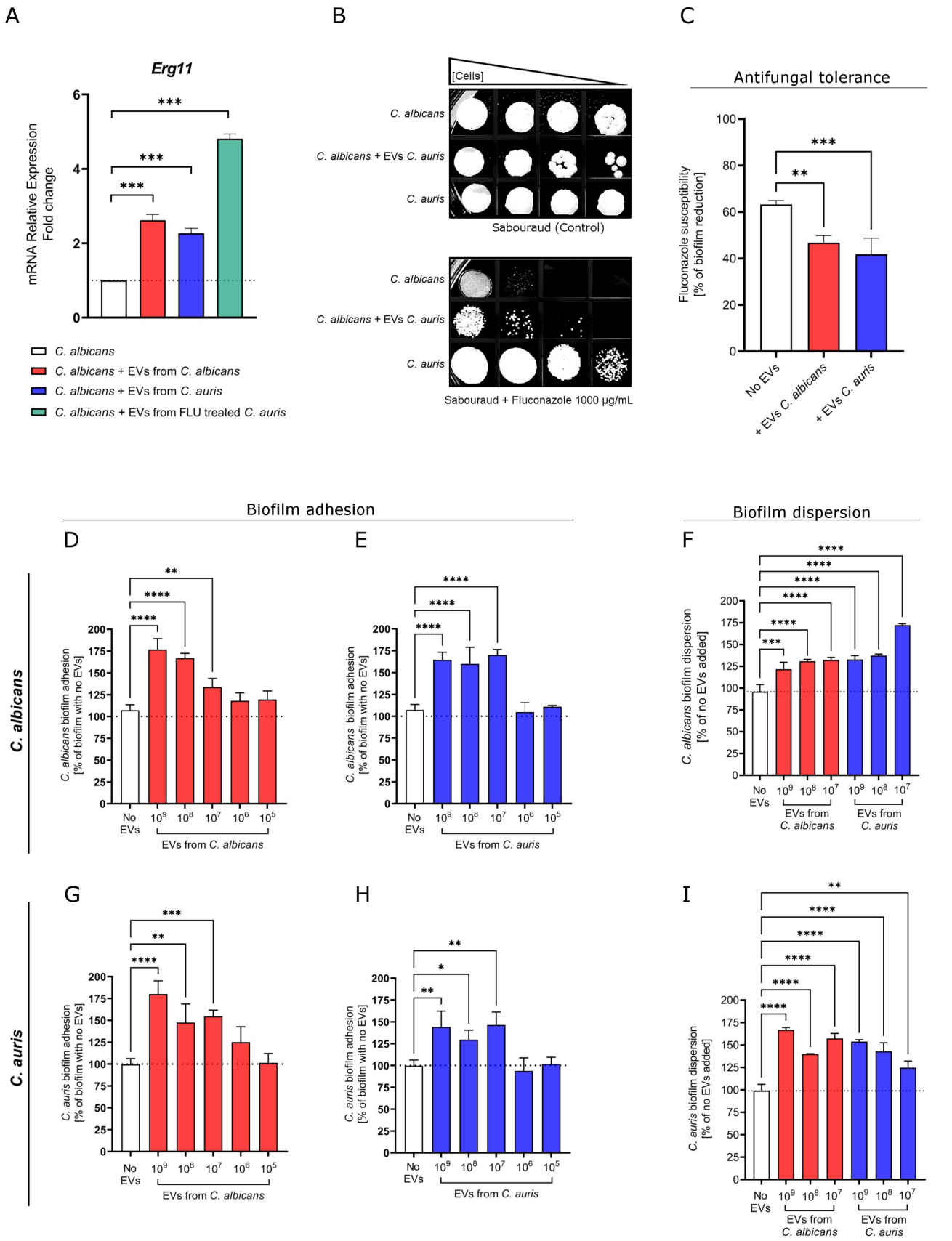
E

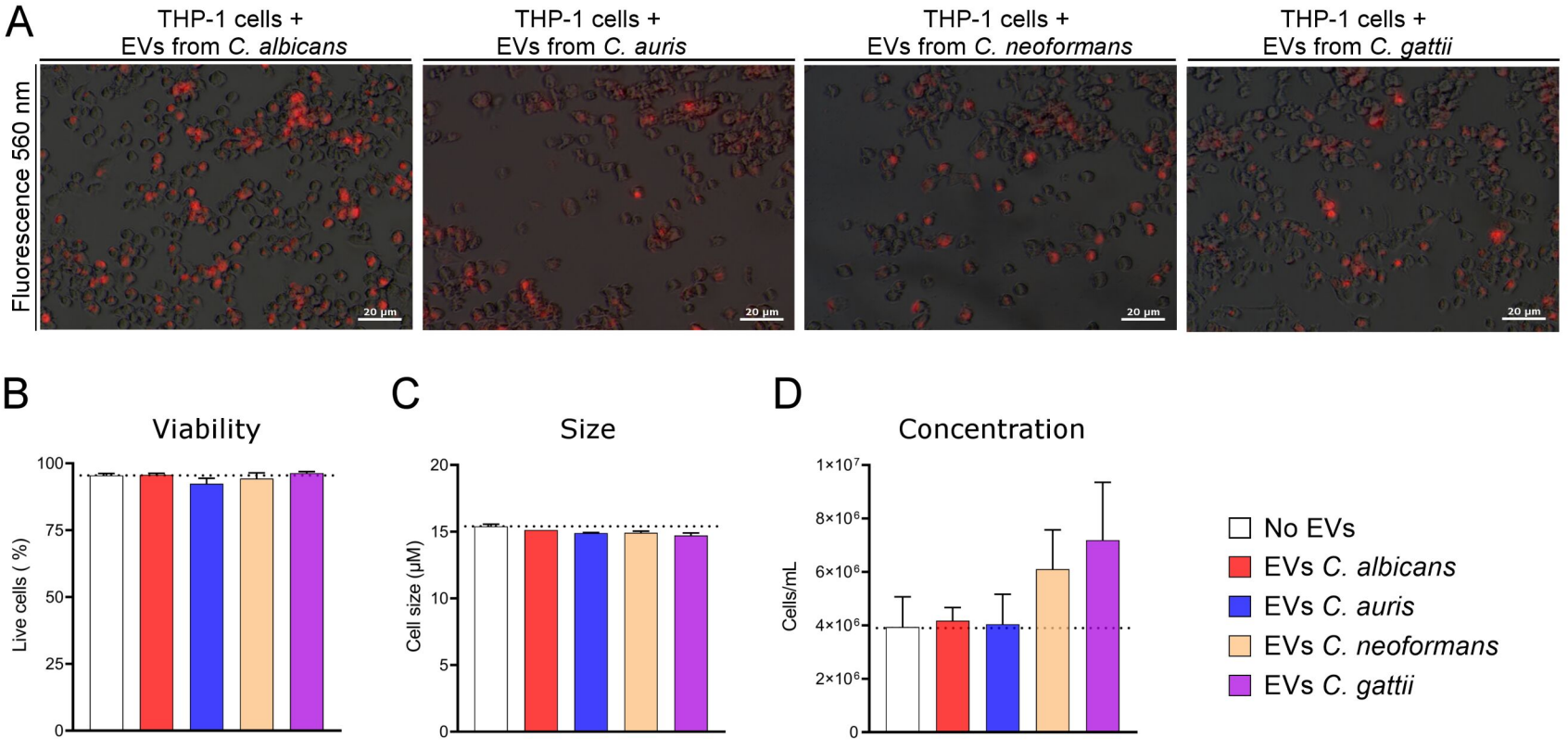
Strain	EVs mean size	EVs mode size	EV/cell ratio
C. albicans ATCC 64548	172 nm ± 64 nm	136 nm	3,6 ± 3,5 EVs/cell
C. auris 470/2015	137 nm ± 67 nm	99 nm	3,9 ± 3,3 EVs/cell
C. neoformans H99	198 nm ± 92 nm	148 nm	1,5 ± 1,0 EVs/cell
C. gattii R265	204 nm ± 99 nm	137 nm	1,7 ± 1,4 EVs/cell

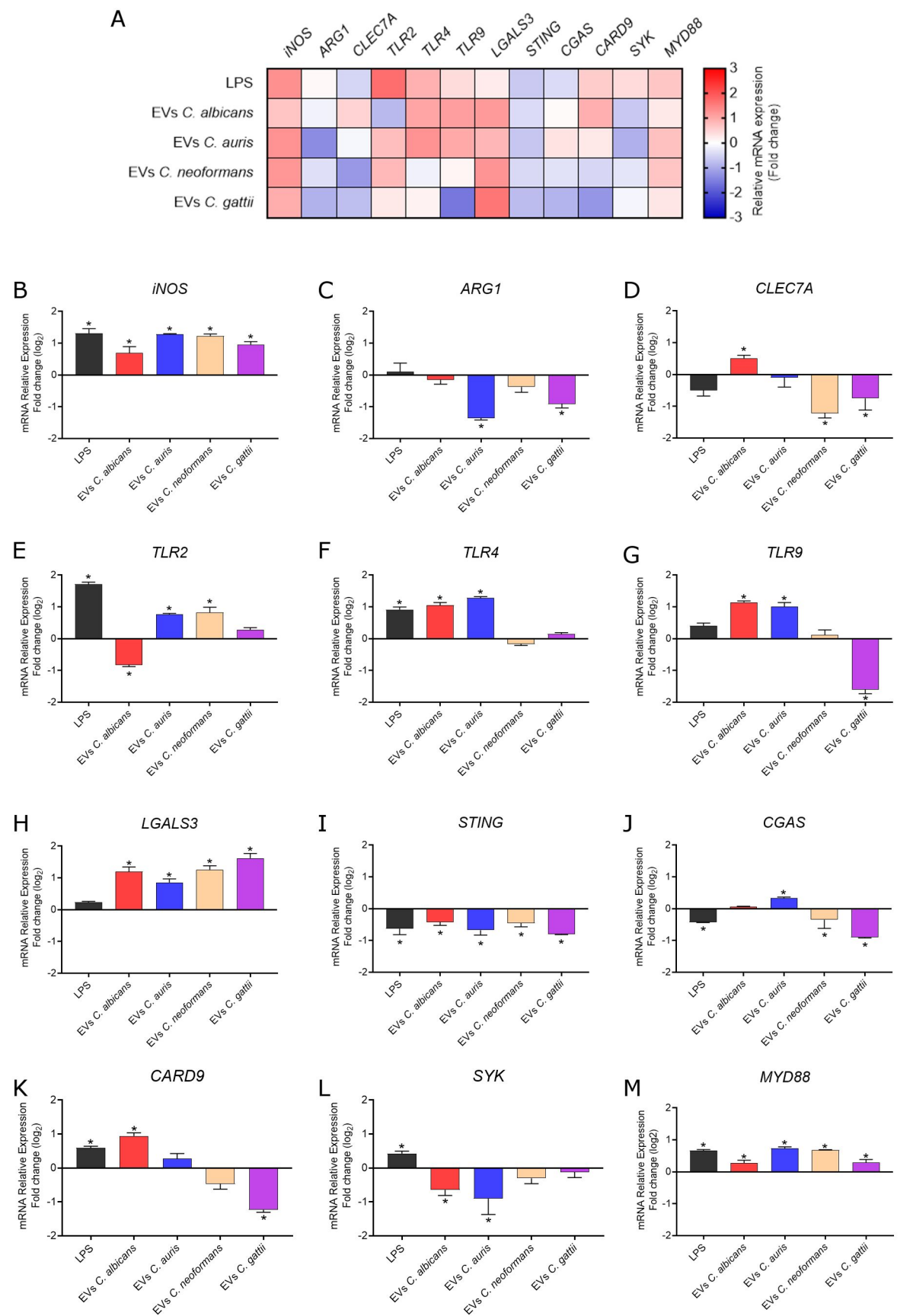


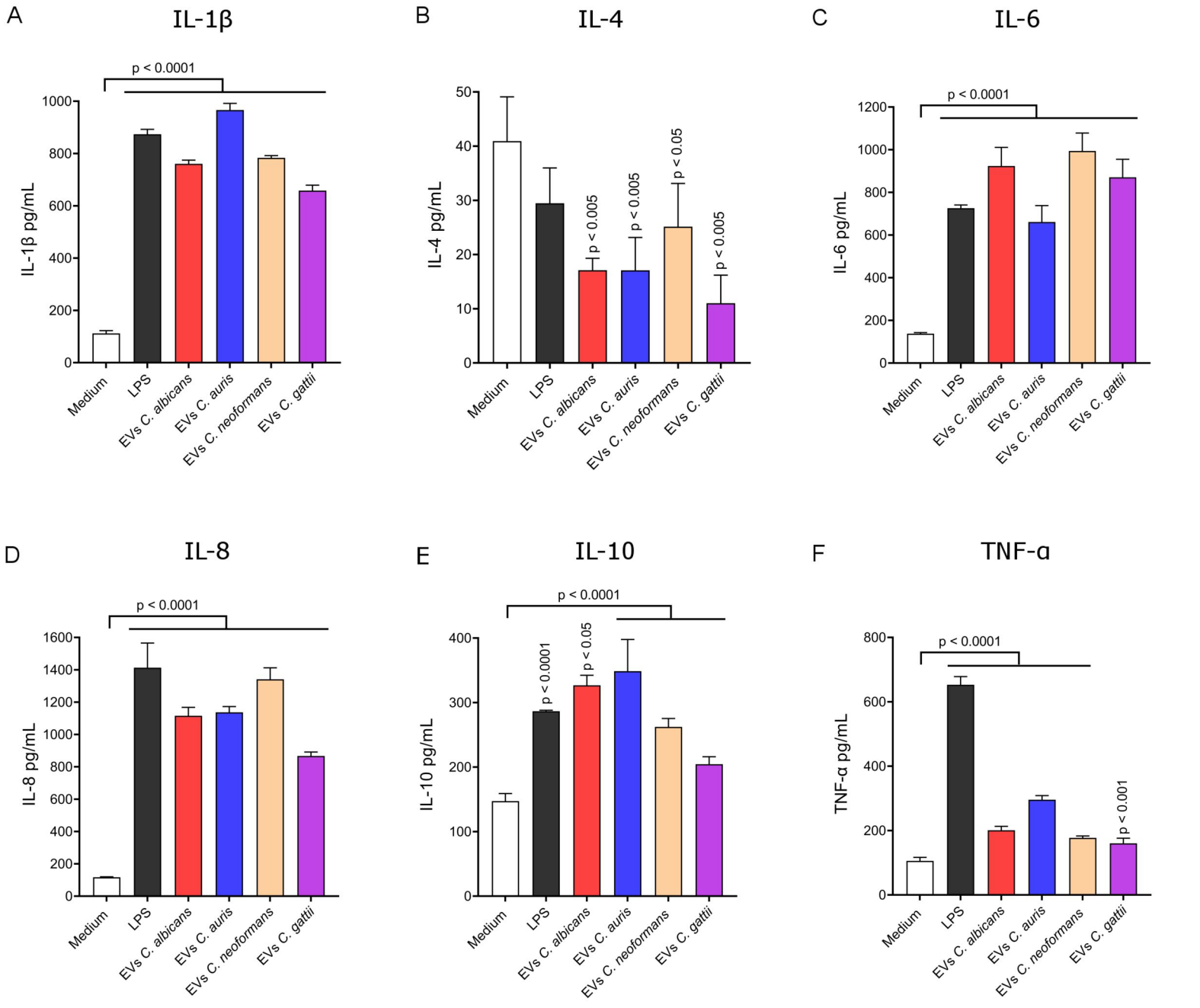

A
Bright field
Fluorescence 560nm
Merged
C. albicans + C. auris EVs
C. gattii + C. neoformans EVs
C. auris + C. neoformans EVs
20 µm
B
C. albicans
C. albicans + C. auris EVs
C
C. neoformans ΔCap67
ΔCap67 + C. gattii EVs
1µm


A
Cap59
mRNA Relative Expression
Fold change
B
Lac1
C
Ure1
D
[EVs]
EVs C. neoformans ΔCap67
EVs C. neoformans H99
EVs C. gattii R265
-
Cn
Cg
E
[Cells]
C. neoformans ΔCap67
ΔCap67 + EVs C. neoformans H99
ΔCap67 + EVs C. gattii R265
C. neoformans H99
C. gattii R265
C. neoformans ΔCap67
C. neoformans ΔCap67 + EVs C. neoformans ΔCap67
C. neoformans ΔCap67 + EVs C. neoformans
C. neoformans ΔCap67 + EVs C. gattii
Biofilm adhesion
F
ΔCap67 biofilm adhesion
[% of no EVs added]
No EVs
EVs from
C. neoformans ΔCap67
G
EVs from
C. neoformans H99
H
EVs from
C. gattii R265
I
Biofilm dispersion
C. neoformans ΔCap67 biofilm dispersion
[% of no EVs added]
No EVs
+ EVs C. neoformans Cap67Δ
+ EVs C. neoformans H99
+ EVs C. gattii R265
J
Antifungal tolerance
Fluconazole susceptibility
[% of biofilm reduction]
Fluconazole
Amphotericin B
C. neoformans ΔCap67 (No EVs)
C. neoformans ΔCap67 + EVs C. neoformans
C. neoformans ΔCap67 + EVs C. gattii
K
[Cells]
ΔCap67 + EVs C. gattii R265
ΔCap67 + EVs C. neoformans H99
C. neoformans ΔCap67
Sabouraud (Control)
Sabouraud + Fluconazole 6 µg/mL


A
Erg11
mRNA Relative Expression
Fold change
C. albicans
C. albicans + EVs from C. albicans
C. albicans + EVs from C. auris
C. albicans + EVs from FLU treated C. auris
B
[Cells]
C. albicans
C. albicans + EVs C. auris
C. auris
Sabouraud (Control)
Sabouraud + Fluconazole 1000 µg/mL
C
Antifungal tolerance
Fluconazole susceptibility
[% of biofilm reduction]
No EVs
+ EVs C. albicans
+ EVs C. auris
Biofilm adhesion
Biofilm dispersion
C. albicans
C. auris
C. albicans biofilm adhesion
[% of biofilm with no EVs]
C. albicans biofilm dispersion
[% of no EVs added]
C. auris biofilm adhesion
[% of biofilm with no EVs]
C. auris biofilm dispersion
[% of no EVs added]
No EVs
EVs from C. albicans
EVs from C. auris


A
THP-1 cells + EVs from C. albicans
THP-1 cells + EVs from C. auris
THP-1 cells + EVs from C. neoformans
THP-1 cells + EVs from C. gattii
Fluorescence 560 nm
20 µm
B
Viability
Live cells (%)
100
75
50
25
0
C
Size
Cell size (µM)
20
15
10
5
0
D
Concentration
Cells/mL
1×10⁷
8×10⁶
6×10⁶
4×10⁶
2×10⁶
0
No EVs
EVs C. albicans
EVs C. auris
EVs C. neoformans
EVs C. gattii


A
iNOS
ARG1
CLEC7A
TLR2
TLR4
TLR9
LGALS3
STING
CGAS
CARD9
SYK
MYD88
LPS
EVs C. albicans
EVs C. auris
EVs C. neoformans
EVs C. gattii
Relative mRNA expression (Fold change)
B
iNOS
C
ARG1
D
CLEC7A
E
TLR2
F
TLR4
G
TLR9
H
LGALS3
I
STING
J
CGAS
K
CARD9
L
SYK
M
MYD88
mRNA Relative Expression Fold change (log2)


A
IL-1β
p < 0.0001
IL-1β pg/mL
1000
800
600
400
200
0
Medium
LPS
EVs C. albicans
EVs C. auris
EVs C. neoformans
EVs C. gattii
B
IL-4
IL-4 pg/mL
50
40
30
20
10
0
p < 0.005
p < 0.005
p < 0.05
p < 0.005
C
IL-6
p < 0.0001
IL-6 pg/mL
1200
1000
800
600
400
200
0
D
IL-8
p < 0.0001
IL-8 pg/mL
1600
1400
1200
1000
800
600
400
200
0
E
IL-10
p < 0.0001
IL-10 pg/mL
400
300
200
100
0
p < 0.0001
p < 0.05
F
TNF-α
p < 0.0001
TNF-α pg/mL
800
600
400
200
0
p < 0.001